STUDY OF FLAME INHIBITION AND VAPOR RELEASE BY MICROENCAPSULATED FIRE RETARDANT COMPOUNDS

By B. K. Wesley Copeland, Guenther von Elbe, Edward T. McHale, and Clayton Huggett

September, 1969

Prepared under Contract No. NAS2-4988 by
ATLANTIC RESEARCH CORPORATION
A Division of The Susquehanna Corporation
Alexandria, Virginia

for

AMES RESEARCH CENTER

NATIONAL AERONAUTICS AND SPACE ADMINISTRATION

FOREWARD

This report was prepared for the Chemical Research Projects Office (Dr. John A. Parker, Chief) of Ames Research Center, National Aeronautics and Space Administration by the Kinetics and Combustion Group of the Propulsion Division of Atlantic Research Corporation, a Division of the Susquehanna Corporation. Dr. Domenick E. Cagliostro served as Technical Monitor for the program. Work on the contract was completed in May, 1969.

STUDY OF FLAME INHIBITION AND VAPOR RELEASE BY MICROENCAPSULATED FIRE RETARDANT COMPOUNDS

CONTENTS

STUDY OF FLAME INHIBITION AND VAPOR RELEASE BY MICROENCAPSULATED FIRE RETARDANT COMPOUNDS

By B. K. Wesley Copeland, Guenther von Elbe,
E. T. McHale, and Clayton Huggett
Atlantic Research Corporation

SUMMARY

This program was undertaken to support the development by the NASA Ames Research Center of fire resistant structural materials based on microencapsulated fire extinguishing agents incorporated into polymeric matrixes. Specific tasks included the evaluation of a series of agents for efficiency in flame extinguishment and a study of agent release from microcapsules. A survey of chemical extinguishing agents and the mechanism of extinguishment has been published as a separate report (ref. 4).

A series of organohalogen extinguishing agents were evaluated in the propane/air diffusion flame in an opposed jet burner. This method of evaluation was selected since it permitted introduction of the extinguishing agent from the fuel side of the diffusion flame, simulating the mode of action of the microcapsules in a fire situation. Significant differences in behavior were observed when the agent was introduced from the fuel side and from the air side of the burner. Of the agents studied, bromoform ($CHBr_3$) showed the best efficiency on a weight or volumetric basis. Its properties appear to be compatible with the microcapsule technique of application.

Volatile agents escape slowly from the microcapsules under ambient storage conditions by a permeation process. The rate of permeation depends on the specific chemical structure of agent and encapsulant. Carbon tetrabromide diffuses readily through the capsule wall while more volatile materials such as $CF_2ClCFCl_2$ are lost very slowly.

On rapid heating, as when exposed to a fire, the microcapsules rupture due to internal pressure. Capsules will withstand internal pressures of the order of 100 to 200 psi. The samples of microencapsulated agent examined were quite heterogeneous with respect to particle size and wall thickness, resulting in considerable scatter in agent release properties.

INTRODUCTION

Recent research performed at the Ames Research Center of the National Aeronautics and Space Administration has led to significant advances in the state-of-the-art of fire protection materials. Polymeric foams and coatings have been developed which exhibit extremely favorable flame resistant, fire suppressant, and insulative properties for use in aircraft structures and other applications. In one system under study, fire suppressing agents are encapsulated in polymeric microspheres and incorporated into fire resistant foams. When such a material is exposed to the heat from a fire, the agent is released, extinguishing the fire.

Among the advantages of such a system we may note the following:

(a) Conventional, well characterized, and readily available polymers may be used with minimal effects on their properties due to the incorporation of additives in encapsulated form.

(b) The fire suppressing agent is released directly into the fire zone where it can act with maximum effectiveness. The quantity of agent released in a fire is kept to a minimum, reducing the associated hazards of toxicity and corrosion.

(c) The agent is released automatically in the event of a fire. Detection and dissemination systems are unnecessary and the possibilities of premature actuation or failure to actuate are eliminated.

(d) The choice of fire extinguishing agents is broadened since limitations on physical properties inherent in conventional agent dissemination systems no longer apply.

The present program was undertaken to support the development and application of microencapsulated fire extinguishing agents through studies of the relative efficiencies of candidate agents, the release of agent from the microcapsules when exposed to a heat source, and the mode of interaction of the agent with the flame.

EVALUATION OF EXTINGUISHING AGENTS

Previous investigations have demonstrated the feasibility of obtaining a measure of flame strength in a diffusion flame by determining the critical flow velocity at which a flame between opposing jets of fuel and air is extinguished at the stream center (ref. 1, 2, 3). In the present work this method has been used to obtain a rating of the relative efficiency of a number of extinguishing agents by measuring the decrease in flame strength on addition of agent vapor to propane fuel.

This method of evaluating inhibitor efficiency was selected for the present study because it permits introduction of the agent from the fuel side of a diffusion flame. This simulates the manner in which agent would be introduced into the combustion zone in an actual fire involving a polymeric material containing an encapsulated extinguishing agent. The more common technique for evaluating extinguishing agent efficiency makes use of the measurement of the reduction in flame speed on addition of agent to a premixed flame.[a] This method does not provide a good simulation of a fuel-air fire which is largely diffusion controlled. It should also be noted that conventional fire extinguishment systems introduce the extinguishing agent from the air side of the fire where only a small part of the total agent charge may reach the combustion zone.

---

[a]Methods of determining inhibitor effectiveness have been reviewed in a recent report prepared under this contract. (Ref. 4).

Experimental Results

The flame strength in the opposed jet burner N_f is defined as:

$$N_f = \frac{\text{critical fuel flow in fuel-plus-agent stream}}{\text{critical fuel flow in agent-free fuel stream}} \qquad (1)$$

It will be shown in the following section that N_f, as defined above, is a valid measure of the effect of the inhibiting agent on the fuel consumption rate. When N_f is plotted vs. volume fraction of agent in the fuel stream an approximate straight line with a negative slope is obtained. At high concentrations of agent the flame becomes unstable, the line may show curvature, and eventually the flame is extinguished.

An additive which acts primarily as an inert diluent will show a slope of ≈ -1 since the total volumetric flow of (fuel + agent) remains almost unchanged by the addition of the agent. We therefore take the quantity

$$n = -[1 + \Delta N_f/\Delta(\text{volume fraction agent})] \qquad (2)$$

as a ranking parameter for comparison of the effectiveness of chemical extinguishing agents. This choice of defining a ranking parameter has the advantage of emphasizing the chemical effectiveness of inhibiting agents while tending to exclude the physical component of the effect.

Results of the agent evaluation measurements are summarized in Table I below. Complete data on all runs are given in the Appendix (Table AI). Best straight lines were drawn visually through the data points of Table AI and were used in the calculations of slopes for determining n-values, even though, as noted above, some curvature of the lines usually became prominent at the high additive levels.

The agents of Table I fall into three groups: the highly brominated compounds which have relatively high values of n and are superior inhibitors; those agents with values of n near unity which exhibit moderate chemical inhibiting effectiveness; and those compounds with n-values near zero which act only as diluents. The scatter of the experimental data points sets the limits of precision of the ranking, and this scatter as judged from composite plots of the results indicates that complete confidence can be put in the groupings given above. The data for three selected agents, one from each

group, are plotted in figure AI to illustrate this point. However, the data are not precise enough to allow one to reliably distinguish between members of any one group. For example, within statistical error, CCl_3Br is probably not superior to CCl_4.

Table I

Summary of Inhibitor Ranking Parameter Values

Agent	η
$CHBr_2CHBr_2$	3.2
$CHBr_3$	2.9
CBr_4	2.9
CCl_3Br	1.4
CH_3Br	1.3
CF_2BrCF_2Br	1.3
CCl_4	1.1
CF_3Br	1.0
SO_2	0.1
H_2O	-0.03
$CF_2ClCFCl_2$	-0.28

Measurements were made at approximately 110°C in most cases. Where the vapor pressure of the inhibitor was too low to give effective concentration at this temperature, a temperature of about 200°C was used. Experiments with CF_2BrCF_2Br suggest that the measured value of η may increase somewhat with temperature.

The use of η permits a comparison of the effectiveness of different agents at equal molar concentrations in the fuel stream. This is useful in discussing the effect of molecular structure on inhibitor action. A value of $\eta \approx 0$ indicates that the agent is acting primarily as an inert diluent. Water vapor, SO_2, and $CF_2ClCFCl_2$ appear to act largely in this way. Larger values of η indicate chemical inhibiting effects on the flame, the larger

the value of n the greater the inhibitor effectiveness on a molar basis.

The importance of bromine to effective inhibitor action is confirmed by the data of Table I. On the other hand, the relative inefficiency of fluorine containing compounds in the present experiments was unexpected. Both CF_3Br and CF_2BrCF_2Br are reported to be effective inhibitors in premixed flames and even $CF_2ClCFCl_2$ shows significant activity. The effect of chemical structure on inhibitor efficiency is discussed in greater detail in a later section.

From a practical standpoint, the inhibitor effectiveness per unit weight or per unit volume of inhibitor in the condensed phase is of interest. Relative efficiencies calculated in these two ways are summarized in Table II.

Mass and Volume Rankings of Inhibitors

Agent	Molar Rank η	Mass Rank $x10^3$ $\eta/M.W.$	Volume Rank $x10^3$ $\eta\rho/M.W.$
$CHBr_2CHBr_2$	3.2	9.3	27.6
$CHBr_3$	2.9	11.5	33.4
CBr_4	2.9	8.7	30.0
CCl_3Br	1.4	7.1	13.8
CH_3Br	1.3	13.7	a
CF_2BrCF_2Br	1.3	5.0	10.8
CCl_4	1.1	7.2	11.4
CF_3Br	1.0	6.4	a
SO_2	0.1	1.6	a
H_2O	-0.03	-1.7	-1.7
$CF_2ClCFCl_2$	-0.28	-1.5	-2.3

a = Gas at normal temperature and pressure

The former permits a ready comparison of the relative cost of various inhibitor systems, while the latter allows an estimate of the volume fraction of microencapsulated agent which must be added to the base polymer to provide fire suppression action. A small volumetric loading will be desirable to minimize effects on the physical properties of the polymer.

Addition of inhibitor to the air stream. - A few experiments were carried out in which the agent was introduced into the air stream rather than the fuel stream (data in Appendix). Sulfur dioxide appeared to be roughly four times more effective when introduced in the air stream. In the case of $C_2F_4Br_2$ small concentrations in air were somewhat more effective than in the fuel, but as the concentration in air was increased the flame quickly became unstable and no reliable value of inhibitor efficiency was obtained. Similar effects have been observed previously when methyl bromide was added to a diffusion flame (ref. 6, 7). When it is considered that a stoichiometric propane-air flame requires approximately 24 volumes of air per volume of propane, it appears that the total quantity of inhibitor required to control a fire may be smaller and the true inhibitor efficiency greater when the inhibitor is introduced with the fuel.

Attempted evaluation of tris (2,3-dibromopropyl) phosphate. - This compound has a vapor pressure of 4 torr at 250°C. In an attempt to obtain an effective concentration in the fuel stream in the form of vapor or aerosol, it was injected into a high temperature vaporizer in the fuel line by means of a motor driven syringe. The agent could not be driven off the evaporator without the onset of extensive decomposition. The temperature was varied up to 476°C, at which point heavy carbonaceous deposits on the evaporator completely blocked the addition of more agent. Since it is generally thought that bromine is the active inhibiting species of most compounds that exhibit flame inhibition, we attempted to allow the tris compound to decompose and to evaluate the effect of the decomposition products on the flame. This produced only an orange color in the flame, but no detectable change in flame strength. Because the decomposition products were mainly solids left behind in the evaporator, no concentration value could be reported.

Analysis of combustion products. - An attempt was made to analyze for inhibitor fragments in the combustion products from the burner. Samples of the burner effluent were collected in heated glass sampling bulbs and

introduced into the inlet of a quadrupole mass spectrometer. When CBr_4 was introduced into the fuel stream without a flame the expected fragment pattern was obtained. (Figure 1). However, no bromine containing fragments could be found in the exhaust products from the burner flame. The failure to find HBr was not unexpected, since it is known to be difficult to detect with the mass spectrometer in this type of experiment (ref. 8,9), but since only a small part of the fuel was consumed in the burner it was expected that a part of the CBr_4 would survive.

In another preliminary experiment the exhaust products from a flame containing CCl_3Br were studied with the mass spectrometer. Fragments containing chlorine bonded to carbon appeared to be present but no bromine containing species were identified. Further analytical studies of inhibitors containing chlorine or fluorine in addition to bromine would appear to be of interest.

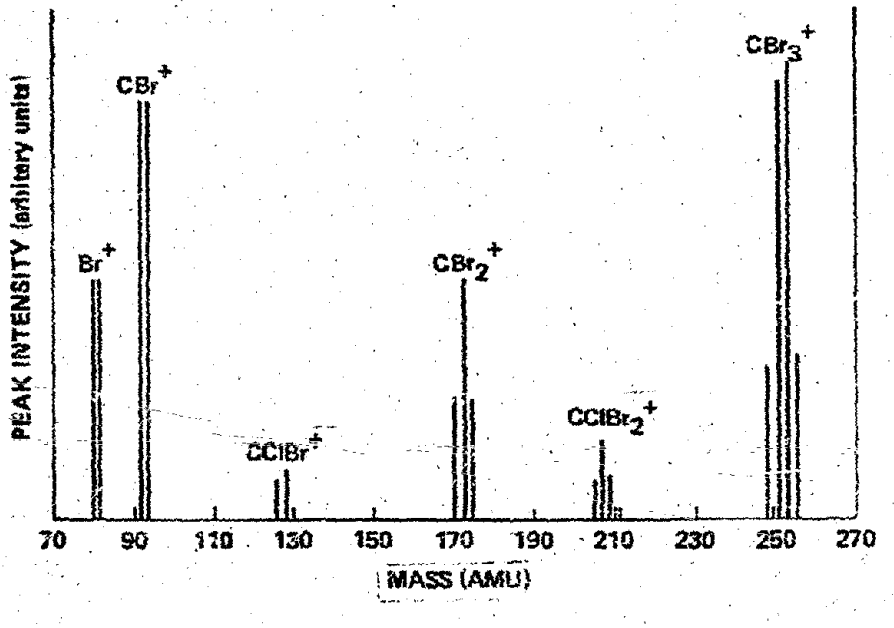

Figure 1
Mass Spectrum of CBr_4 in Propane Stream
(Trace of $CClBr_3$ impurity)

Theory of Flame Strength in the Opposed Jet Burner

It has been pointed out by Potter and co-workers (ref. 1 and 2) that the critical flow for disrupting the diffusion flame between opposed fuel and oxidant jets characterizes the rate of the chemical reaction in the flame zone; thus, the index of flame strength derived from the critical flow is considered to be an index of the effect of inhibiting agents on the intensity of the combustion reaction. However, there are three flow parameters in the present experiments, i.e., the flow of propane, the flow of propane plus admixed agent vapor, and the flow of air, and the experimental data show that these flows are not equivalent: substantially different and contradictory ratings of agent efficiencies are obtained if the flow of propane plus agent or the flow of air is substituted for the flow of propane in the index of flame strength formulated by equation 1. It is therefore necessary to examine which flow bears a meaningful relation to the reaction rate in the flame zone; otherwise the validity of the method and the relevancy of the data are open to question.

Let us consider a diffusion flame between parallel streams of fuel and air, as shown schematically in figure 2. As the two streams pass the edge of the dividing partition they interdiffuse and the opposing diffusion flows of fuel and O_2 react to yield the products CO_2 and H_2O. Thus, a zone of chemical reaction is maintained which is bound on the right by a surface in which the fuel consumption is completed and on the left by a surface in which the consumption of O_2-molecules is completed. No fuel exists on the right side and no O_2 exists on the left side of the reaction zone, but mass conservation is preserved by the products CO_2 and H_2O which diffuse in both directions, and by the atmospheric nitrogen which continues to interdiffuse with the fuel gas.

The positions of the reaction zone boundaries are determined by the condition that the diffusion flow of fuel across the left-side boundary is in stoichiometric proportion to the flow of O_2 across the right-side boundary, and by the further condition that the distance between the

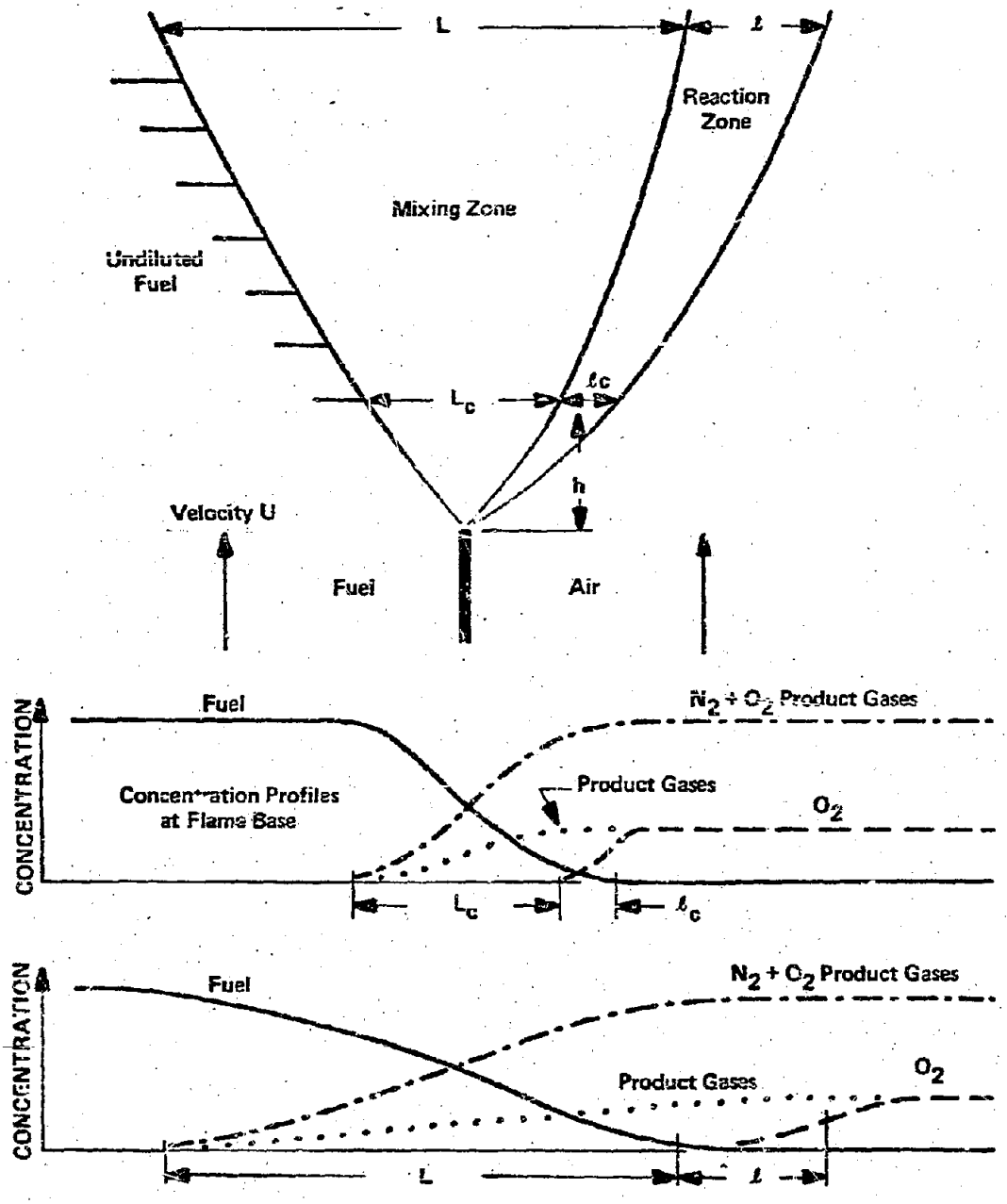

Figure 2
Scheme of Diffusion Flame Between
Parallel Streams of Fuel Gas and Air

boundaries is determined by the rate of the chemical reaction, in the sense that the consumption of either component is completed in the time of travel from one boundary to the other.

Taking the fuel to be propane and using simple dimensional analysis, we may represent the flux of propane into the reaction zone by $D_p[P]^*/\ell$, where D_p is the diffusion coefficient, $[P]^*$ is a concentration characteristic of the propane concentration at the left-hand boundary of the reaction zone, and ℓ is a length characteristic of the width of the zone. For the flux of O_2 across the other boundary we write similarly $D_{O_2}[O_2]^*/\ell$, and hence

$$D_p[P]^*/\ell = 0.2D_{O_2}[O_2]^*/\ell \qquad (3)$$

since 0.2 moles of propane are required for combustion of one mole O_2. The concentration $[O_2]^*$ cannot exceed the concentration of oxygen in air; and since the molar concentration of air is equal to the molar concentration $[P]_o$ in the diluted propane stream (pressure and temperature being equal), it follows that

$$[O_2]^* \leq 0.21[P]_o \qquad (4)$$

or from equation (3)

$$[P]^*/[P]_o < 0.042(D_{O_2}/D_p) \qquad (4a)$$

which shows that the propane concentration $[P]^*$ at the reaction zone boundary is a very small fraction of the concentration $[P]_o$, inasmuch as the diffusivity ratio D_{O_2}/D_p is of the order of unity. This means that the reaction zone is situated beyond the boundary of the fuel stream at the extreme tail-end of the propane concentration profile where the consumption of propane in the reaction zone has very little effect on the shape of the profile at higher levels of concentration. The propane flux is therefore substantially governed by diffusion without chemical reaction, and the oxygen flux adjusts itself to the propane flux according to the above stoichiometric relations, supplemented by

$$D_p[P]_o/L = D_p[P]^*/\ell \qquad (5)$$

which represents the continuity of flux across the reaction zone boundary, L being a length characteristic of the length of the propane concentration profile.

The rate of the chemical reaction is introduced by the equation

$$D_p[P]^*/\ell = \bar{r}\,\ell \qquad (6)$$

where $\bar{r}$ is the average rate of propane consumption in moles per unit volume and unit time. The further relation

$$\bar{r} = f(\,[P]^*,\ [O_2]^*,\ \bar{T},\ [\bar{R}]\,) \qquad (7)$$

shows $\bar{r}$ to be a function of the concentrations of propane and oxygen, the average temperature $\bar{T}$ and the average free-radical concentration $[\bar{R}]$ in the reaction zone. The magnitude of each of these parameters, and hence of $\bar{r}$, is restricted by kinetic and thermodynamic bounds. All of these parameters decrease in the process of interdiffusion of the streams, that is at increasing distance from the flame base. It is therefore probable that $\bar{r}$ decreases at a higher order than $[P]^*$, and since from equation (6)

$$\ell = \sqrt{D_p[P]^*/\bar{r}} \qquad (8)$$

the width of the reaction zone increases with increasing distance from the flame base, as indicated schematically in figure 2. At the flame base the value of $\bar{r}$ and $[P]^*$ are at a maximum. According to equation (4), approximately,

$$[P]^*_{max} = 0.042\ (D_{O_2}/D_p)\ [P]_o \qquad (9)$$

and from (5), (6), and (9) the maximum (or critical) flux of propane at which the reaction is sustained becomes

$$D_p[P]_o/L_c = \sqrt{0.042\ D_{O_2}[P]_o\ \bar{r}_{max}} \qquad (10)$$

The flux decreased from "infinity" at the point of entrance of the stream into the mixing zone, i.e., at the burner exit, to the critical flux

$D_p[P]_o/L_c$ at the height h above the burner exit. If U is the stream velocity and τ is the time in which the flux decreases from "infinity" to the critical value, the height of the flame base above the burner is given by

$$h = U\tau \tag{11}$$

The time τ and the diffusion distance L_c are related roughly by the equation

$$L_c^2 = 2 D_p \tau \tag{12}$$

and combining equations (10), (11), and (12) one obtains

$$\bar{r}_{max} = 12 \frac{D_p}{D_{O_2}} \frac{1}{h} \times U[P]_o \tag{13}$$

The product $U[P]_o$ is the fuel flow. If an agent is added to the stream which decreases $\bar{r}_{max}$, and if the fuel flow is unchanged, the flame height h increases according to equation (13). If the fuel flow is decreased until the former flame height is reestablished, one obtains from equation (13)

$$\frac{\bar{r}_{max} \text{ with agent}}{\bar{r}_{max} \text{ without agent}} = \frac{\text{fuel flow with agent}}{\text{fuel flow without agent}} = N_f$$

which shows that the index of flame strength, as defined by equation (1), is indeed a measure of the decrease of the reaction rate in the flame zone.

It is experimentally possible to maintain a lifted flame and obtain data on N_f from flame height observations, but the method is not attractive because the gas velocity U has an awkward and variable profile at the stream boundary. In particular, immediately at the burner rim the velocity is zero, so that the flame tends to settle there. It is therefore far more practicable to use the opposed-jet method which utilizes the stable center portions of well-developed Poiseuille flow profiles in the counterflowing streams of fuel gas and air.

The method is illustrated schematically in figure 3. The impingement of the jets produces a stagnation point which fixes the diffusion

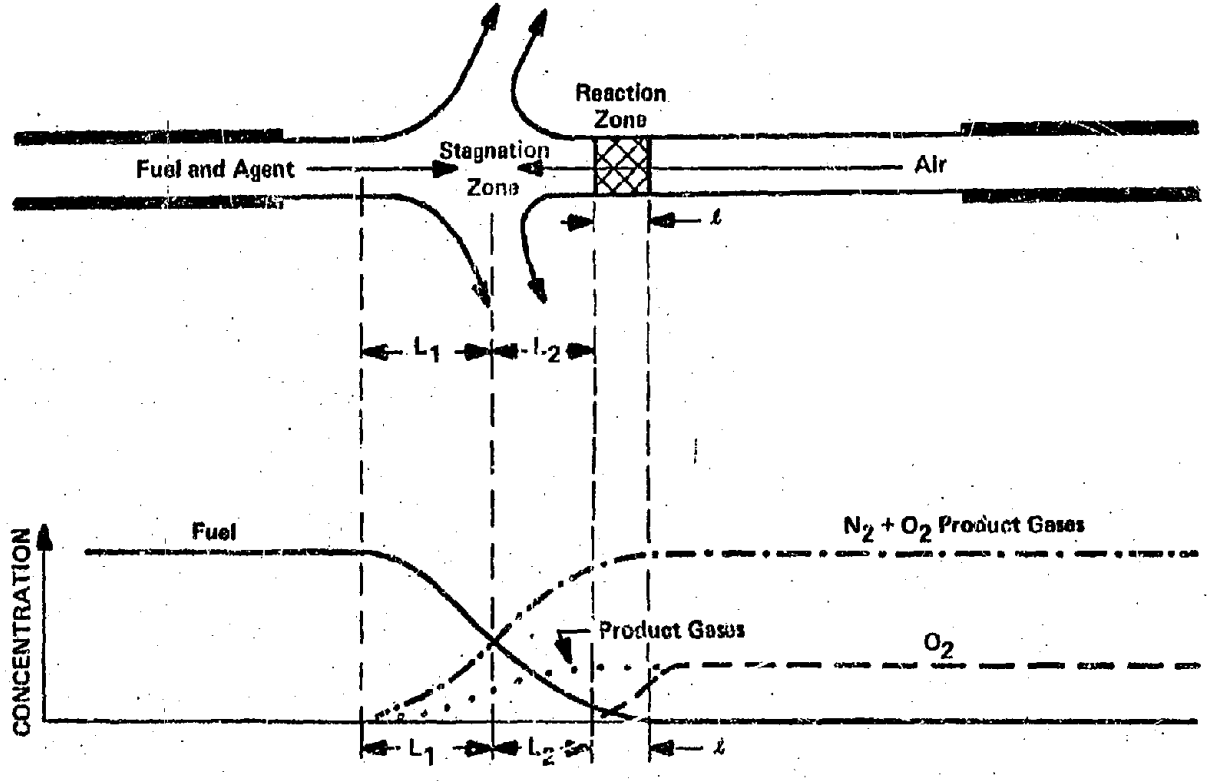

Figure 3
Schematic of Diffusion Flame Between
Opposing Streams of Fuel and Air

interface between the streams. The air and fuel streams may be so adjusted that the reaction zone is equidistant from the stream outlets; thus, the stagnation zone is located off-center toward the fuel outlet because the reaction zone is situated at the extreme tail-end of the fuel concentration profile on the air-side of the diffusion interface, as has been discussed above. A particle suspended in the air stream passes through the flame whereas a particle suspended in the fuel stream does not; a fact that has been demonstrated experimentally by Potter and co-workers (2). The off-center position of the stagnation zone signifies that the momentum of the air stream $\rho_{air} U^2_{air}$ (ρ= density, U = linear velocity), is larger than the momentum $\rho_F U^2_F$ on the fuel side (ρ_F being the density of the fuel/agent mixture). In the present experiments the momentum ratio is found to be always close to 2. We mention here that by using ethane, oxygen and nitrogen one can prepare ethane/nitrogen and oxygen/nitrogen mixtures of virtually identical diffusivities and densities and a stoichiometric ratio of 1:1 by volume. In opposing streams of such mixtures of equal velocities the stagnation zone and the reaction zone coincide exactly at equal distances from the stream outlets and particles suspended in either stream do not pass through the flame. This has been demonstrated experimentally by Pandya and Weinberg (10). But in the usual hydrocarbon-air diffusion flames the reaction zone is always on the air side of the diffusion interface, and since in the opposed-jet configuration air enters the reaction zone virtually undiluted by combustion products, the concentration $[O_2]^*$ is always $0.21[Air]_o$, where $[Air]_o$ denotes the concentration of molecules of nitrogen and oxygen in undiluted air. Thus, from equation (3),

$$[P]^* = 0.042\ (D_{O_2}/D_p)\ [Air]_o \qquad (15)$$

and from equation (6)

$$\bar{r} = 0.042\ D_{O_2}[Air]_o/\ell^2 \qquad (16)$$

Using the subscript i to denote concentrations at the diffusion interface, we write analogous to equation (5)

$$D_p[P]_i/L_2 = 0.042D_{O_2}[Air]_o/\ell \qquad (17)$$

The term $D_p[P]_i/L_2$ is the diffusion flux of propane across the interface, and since the system is in a steady state this flux is balanced by the outflow of propane at the interface, which is the product of the concentration $[P]_i$ and the velocity of the air stream, U_{air}. We write therefore

$$D_p[P_2]_i/L_2 - [P]_i U_{air} = 0 \qquad (18)$$

Values of U_{air} are obtained from the data in Table 1 by the relation

$$U_{air} = \frac{\text{Air volume flow, cm}^3\text{/sec at 1 atm and test temperature}}{\text{Tube cross section, 0.164cm}^2} \ \frac{\text{cm}}{\text{sec}} \qquad (19)$$

Writing $[Air]_i$ for the concentration of nitrogen and product gases at the interface, the analogous equation for the flux balance on the fuel side becomes (with $D_{Air} = D_{O_2}$)

$$D_{O_2}[Air]_i / L_1 - [Air]_i U = 0 \qquad (20)$$

where U is the velocity of the propane + agent mixture, i.e.,

$$U = \frac{\text{fuel volume flow, cm}^3\text{/sec at 1 atm, and test temperature}}{\text{Tube cross section, 0.164 cm}^2} \times \frac{100}{100 - \%\ \text{agent}} \ \frac{\text{cm}}{\text{sec}} \qquad (21)$$

The net flux of molecules across the interface is zero, so that

$$D_{O_2}[Air]_i/L_1 = D_p ([P]_i + [Ag]_i)/L_2 \qquad (22)$$

where $[Ag]_i$ is the concentration of agent molecules at the interface. The total concentration of molecules is constant, so that

$$[Air]_o = [P]_o + [Ag]_o = [P]_i + [Ag]_i + [air]_i \qquad (23)$$

From equations (18) and (20)

$$L_2 = D_p/U_{air} \qquad (24)$$

and

$$L_1 = D_{O_2}/U \tag{25}$$

Taking

$$[P2]_i + [Ag]_i/([P]_o + [Ag]_o) \approx [P]_i/[P]_o \tag{26}$$

one obtains from the above equations

$$D_p \frac{[P]_i}{L_2} = \frac{U_{air}}{U_{air} + U} [P]_o U \tag{27}$$

and for the critical width ℓ_c of the reaction zone corresponding to the critical velocities U_c and $U_{c(air)}$ at which the flame becomes extinct,

$$\frac{1}{\ell_c} = \frac{U_{c(air)}}{U_{c(air)} + U_c} \frac{[P]_o U_c}{.042 D_{O_2}[Air]_o} \tag{28}$$

and for $\bar{r}_{max} = 0.042 D_{O_2}[Air]_o/\ell^2_c$

$$\bar{r}_{max} = \frac{24}{D_{C_2}[Air]_o} \left(\frac{U_{c(air)}}{U_{c(air)} + U_c} \right)^2 \left([P]_o U_c \right)^2 \frac{\text{molecules}}{\text{cm}^3 \text{sec}} \tag{29}$$

where

$$[P]_o U_c = \frac{2.7 \times 10^{19}}{0.164} \frac{273}{T_{(test)}} \times \text{Propane Flow (table A1)} \frac{\text{molecules}}{\text{cm}^2 \text{ sec}} \tag{30}$$

and finally

$$\sqrt{\frac{\bar{r}_{max} \text{ with agent}}{\bar{r}_{max} \text{ without agent}}} = \frac{\text{Fuel flow with agent}}{\text{Fuel flow without agent}} = N_f \tag{31}$$

if $U_c/U_{c(air)} \sim L_{c,1}/L_{c,2}$ (equations (24) and (25)) is constant. Similarity considerations suggest that the ratio L_1/L_2 is constant, and this is confirmed by the data in Table 1A which show that $U_c/U_{c(air)}$ is constant within the experimental limits.

According to equation (31) the effect of agents on the reaction rate is represented by the square of the flame strength index N_f. Thus, an index of .9 corresponds to a reduction of the rate by approximately 20 percent, and an index of .7 to a reduction by 50 percent.

Although the above system of equations represents a dimensional analysis only, it should yield the correct order of magnitude for the reaction rate $\bar{r}_{max}$. Using values of 6.25 and 10.38 cm^3/sec for the propane and air flows at 104°C (Table A1) and the approximate value of 0.3 cm^2/sec for D_{O_2}, one obtains from equation (29) a value of 10^{23} molecules/cm^3 sec, which represents the maximum possible rate of consumption of propane molecules in the reaction zone. This is the same order of magnitude that is found in combustion waves of stoichiometrically pre-mixed hydrocarbons and air, as is expected a priori, and thus confirms that the theory is substantially correct and that the data on flame strength and agent efficiency are valid.

Effect of Inhibitors on the Diffusion Flame

The chemical mechanism of combustion comprises numerous binary reactions between neutral molecules and free radicals or free atoms. The neutral molecules are oxygen, fuel gas, and intermediate reaction products such as hydrogen, carbon monoxide, olefins, acetylene, and aldehydes. Known free radicals are OH, CHO, and fragments of hydrocarbons or oxygenated hydrocarbons with free valences on a C-atom or O-atom; and the free atoms are H and O. Binary reactions of this type, as for example $H_2 + OH = H + H_2O$ or $C_3H_8 + OH = C_3H_7 + H_2O$, have generally low activation energies and correspondingly occur with high probability in molecular collisions of the respective species if the temperature is high. Reactions between neutral molecules such as the reaction $C_3H_8 + O_2 = C_3H_7 + HO_2$ have high activation energies and correspondingly low probabilities even at flame temperatures. Reaction between a neutral molecule and a free radical results in a transfer of the free valence to another molecular species, and this is repeated in subsequent reactions as illustrated by sequences such as $H_2 + OH = H + H_2O$, $H + O_2 = OH + O$, or alternatively, $H + C_3H_8 = C_3H_7 + H_2$, $C_3H_7 + O_2 = C_2H_5CHO + OH$ (or alternatively $C_2H_5CO + H_2O$, $C_2H_5 + CO + OH$, $C_2H_5 + CO + H_2O$), etc., so that each free valence generates a chain of chemical transformations by which the original molecules of fuel are progressively degraded and oxidized. Chains are broken by destruction of free radicals in recombination reactions such as $H + OH + M = H_2O + M$ (where M is an unspecified "third body") and are initiated by generation of free radicals from neutral molecules. This may occur, say, by monomolecular dissociation of fuel molecules as exemplified by $C_3H_8 = C_2H_5 + CH_3$, or by binary fuel-oxygen reactions exemplified by $C_3H_8 + O_2 = C_3H_7 + HO_2$, or by the well-known chain-branching reaction $H + O_2 = OH + O$, which yields two free valences in the form of a bivalent O-atom in addition to the single free valence of the H-atom, which is preserved in the hydroxyl radical. This chain-branching reaction is generally considered to be the predominant mechanism of free radical generation in hydrocarbon flames (ref. 11). The two valences of the O-atom are transferred to other free-radical species by reactions such as $O + C_3H_8 = OH + C_3H_7$, $O + H_2 = OH + H$ and analogous

reactions of O with various intermediate reaction products. The H atoms required for chain branching are generated by the reactions $O + H_2 = OH + H$, $OH + H_2 = H_2O + H$, $OH + CO = CO_2 + H$ and also, according to available evidence , by monomolecular decomposition of aliphatic free radicals, as for example, $C_3H_7 = C_3H_6 + H$ (ref. 12). The decomposition may also occur in other modes, such as $C_3H_7 = C_3H_5 + H_2$, and appears to be the basic mechanism of "cracking" of paraffin hydrocarbons into olefins, H_2 and other fragments such CH_4. Although these "cracking" reactions are endothermic they occur readily at higher temperatures, and in particular in the presence of traces of oxygen which apparently stimulates cracking by generation of OH radicals.

If fuel and oxygen are premixed the reaction zone propagates as a combustion wave from layer to layer of the mixture at the rate at which diffusion of heat and free radicals from the reaction zone initiates the chemical reaction in the adjacent layer of the mixture. The magnitude of this thermal and molecular diffusion flux is limited by the finite rates of the chemical processes of heat release and free-radical generation, and by the upper limits of temperature and free-radical concentrations imposed by exhaustion of fuel, oxygen, and intermediate reaction products (including free radicals) in the reaction zone. The combustion wave thus attains a steady state in which the various interdependent parameters - the burning velocity, viz., the wave velocity relative to the unburned gas, the temperature profile, the concentration profiles of the various molecular species, and the various chemical rate processes - are in equilibrium. If the gases are not premixed and burn as a diffusion flame a similar equilibrium is maintained between diffusion of fuel and oxygen into the reaction zone, chemical generation of heat and free radicals in the zone, and outward diffusion of heat and free radicals from both sides of the reaction zone into the streams of fuel and oxygen. However, there is no combustion wave or burning velocity associated with the process, and the equilibrium changes continuously downstream from the zone of initial fuel-oxygen contact as the streams become progressively diluted by the reaction products.

Addition of an inert gas decreases the temperature levels throughout the reaction zone due to the heat capacity of the additive. This has both the physical effect of reducing the thermal diffusion flux and the chemical effect of reducing reaction probabilities in molecular collisions according to the activation energies of the various elementary reactions. The overall effect on a premixed flame is a decrease of the burning velocity and an increase of the width of the combustion wave. If the dilution is carried sufficiently far the wave width becomes so large that the temperature and concentration profiles are critically perturbed by the flame-generated gas flow. This flow originates from the thermal expansion of the burning gas and, as discussed in ref. 13, it has shear components parallel to the flame surface depending on confinement and other factors such as buoyancy. The shear flow increases the flux of heat and free-radicals from the reaction zone into the unburned gas, causing extinction of the flame when the diluent percentage exceeds the critical limit known as limit of flammability. A similar critical limit applies to diffusion flames, as has been observed in the present experiments.

Additives such as $CHBr_3$, CH_3Br, etc., are fuels and have a significant diluent effect only if the mixture is deficient in oxygen. They burn in diffusion flames where the supply of oxygen is unlimited. Even CBr_4 is by no means an inert diluent in the sense of N_2 or H_2O since the reaction $CBr_4 + O_2 = CO_2 + 2Br_2$ generates about 106 kcal per mole. The strong inhibiting effect of these compounds is therefore attributable to chemical inhibition of free-radical chains.

An obvious inhibiting reaction is typified by $\equiv CBr + H \rightarrow \equiv C\cdot + HBr$, which is exothermic by about 20-30 kcal/mole and thus should have a high probability of occurrence. This type of reaction inhibits chain branching by capturing H - atoms and thus suppressing the generation of OH and O in reactions of H with O_2. Although it generates free radicals such as CBr_3, $CHBr_2$, etc., the reaction chains originating from these free-radical species are not branched and the overall concentration of free radicals is decreased corresponding to the decrease

of the ratio of chain-branching by $H + O_2 = OH + O$ to chain-breaking by free-radical recombinations. Chain branching is also inhibited if O-atoms are captured in reactions that do not yield chain-continuing atoms or free radicals. In particular, reactions of O with carbon compounds are conceivable in which O and C are double-bonded to C=O and no free valences are generated. Since O-atoms no doubt react very readily with brominated hydrocarbons , one may hypothesize, for example, the occurrence of reactions such as $CBr_4 + O = Br_2CO + Br_2$ (or $CO + 2Br_2$), $CHBr_3 + O = Br_2CO + HBr$, $CH_3Br + O = H_2CO + HBr$, etc. Such reactions would be exothermic of the order of 100 kcal/mole and except for the last reaction would be sufficiently energetic to yield bromine atoms, i. e., $O + CBr_4 = CO + 4Br$, etc. However, bromine atoms are relatively unreactive because reactions such as $C_3H_8 + Br = C_3H_7 + HBr$ are endothermic; hence, if bromine atoms become a significant part of the atom and free-radical population of the system the chain length, viz., the average number of chemical transformations between the generation and destruction of a free valence, is decreased and the overall reaction is slowed down. Thus, the capture of O by a brominated hydrocarbon appears certain to have an inhibiting effect on the chain reaction. The same applies to conceivable reactions of OH such as $CBr_4 + OH = Br_2CO + HBr + Br$, $CHBr_3 + OH = Br_2CO + H_2 + Br$, etc. If fluorocarbons react with oxygen one may expect to obtain the compound F_2CO which is known to be very stable; thus, the reactions $CF_3Br + O = F_2CO + FBr$ and $CF_3Br + OH = F_2CO + HF + Br$ are strongly exothermic and probably take place very readily.

In a diffusion flame of a fuel such as propane in air the flux of air into the reaction zone is about 25 times larger than the flux of propane. Thus, if the inhibitor is admixed to the fuel stream the flux of agent into the reaction zone is much smaller than the flux obtained by admixing an equal percentage of agent to the air stream. It follows that for an equal decrease of the average reaction rate $\bar{r}$ or flame strength index N_f the required agent percentage is higher in the fuel stream than in the air stream. The data in Table AI show that this is the case but that the ratio of agent concentrations in air and

fuel for a given flame strength is of the order of 3 to 4 rather than 25. This supports the concept of a preheat or pre-activation zone situated on the fuel side of the reaction zone, in a region of relatively high fuel concentration. As is well-known, hydrogen and unsaturates are generated on the fuel side of hydrocarbon diffusion flames by endothermic "cracking" induced by the flux of heat and free radicals from the reaction zone (this process generates the characteristic yellow carbon luminosity of flames). The flame is thus maintained by a feedback cycle comprising diffusion of hydrogen from the pre-activation zone into the reaction zone, free-radical generation in the reaction zone via the hydrogen-oxygen chain-branching reaction, heat release in the reaction zone by free-radical chain-reactions, and generation of hydrogen in the pre-activation zone by diffusion of heat and free radicals from the reaction zone. The cycle is disturbed by any agent that disturbs the generation of hydrogen in the pre-activation zone. Hence, if the inhibiting action occurs predominantly in the pre-activation zone, where the concentration of an agent in the fuel stream is relatively high, the agent effect is not nearly as small as would be expected if the inhibition were taking place in the reaction zone. The data thus point to the conclusion that inhibition occurs predominantly in the pre-activation zone.

Further support for this model can be found in the effect of the agent on the position of the reaction zone. Referring to figure 3, the experiment is conducted so that the reaction zone is always kept midway between the opposing orifices. Since the reaction occurs by diffusion of fuel into the air stream, this requires that the stagnation zone must be located on the fuel side of the burner, or that the momentum of the air stream must be greater than that of the fuel stream. This is confirmed by the data in Table III.

TABLE III

EFFECT OF INHIBITING AGENTS ON THE LOCATION OF THE REACTION ZONE

Agent in Fuel		Agent in Air	
% Agent	$\rho U^2_{air}/\rho U^2_{fuel}$	% Agent	$\rho U^2_{air}/\rho U^2_{fuel}$
Agent: CF_2BrCF_2Br			
0.0	1.72	0.0	1.86
3.60	1.54	0.46	2.00
7.56	1.39	0.96	2.07
15.12	1.13	1.13	2.05
18.96	1.05	1.21	2.10
		2.72	2.35
		2.77	2.39
		5.44	flame unstable
Agent: SO_2			
0.0	2.41	0.0	1.42
6.43	2.45	2.32	1.48
9.22	2.29	3.15	1.54
14.50	2.24	3.75	1.60
15.75	2.26	3.80	1.63
18.25	2.28		

However, the data show that when an active inhibitor such as CF_2BrCF_2Br is added to the fuel stream the reaction zone is displaced in the direction of the stagnation zone. As the critical extinction concentration is approached the two zones practically coincide. This must be accompanied by a steepening of concentration and temperature gradients and a narrowing of the reaction zone. Strong aerodynamic forces will contribute to flame instability.

When the agent is added to the air stream the reaction zone is displaced in the opposite direction. This must be accompanied by a lowering of concentration gradients and a broadening of the reaction zone. The volumetric fuel consumption rate falls, the temperature decreases, and eventually the reaction is unable to sustain itself. In this case the concentration gradient of the inhibitor is opposite to that of the radical generating fuel species, causing

a flattening of the reaction profiles, while when the agent is added with the fuel the concentration gradients are in the same direction.

An "inert" diluent such as SO_2 shows only a small effect, although in the same direction. A more detailed study of the structure of the inhibited opposed jet flame should provide important information on the mechanism of inhibitor action.

Similar conclusions have been reached from a study of the inhibition of premixed flames (ref. 9, 14). Although in this case the initial agent distribution is uniform throughout the reaction zone, the principal effect is seen in the pre-activation zone where radical concentrations are suppressed. Concentration and temperature gradients are steepened in the approach to the reaction zone and the maximum flame temperature increases to allow completion of the reaction within the narrower reaction zone.

The heat capacity of SO_2 is larger than the heat capacity of H_2O by a factor of about 1.3, which may explain the somewhat greater efficiency of SO_2 over H_2O as shown in Table 1. The compound $C_2F_3Cl_3$ is not an inert gas but rather a fuel with a calorific value below hydrocarbon fuels. It is therefore an inhibitor but is less efficient than H_2O and SO_2. Bromine compounds may be thought to intercept OH and O that diffuse from the reaction zone into the pre-activation zone and induce "cracking", and also to destroy H generated in the pre-activation zone by reactions such as $H_2 + OH = H_2O + H$. It is noted that in the present work the compound CF_3Br shows up to much less advantage than in previous work (ref. 3) with the opposed-jet burner, in which the fuel was methane and CF_3Br was found to be about as efficient as CH_3Br. The significant difference between a methane and propane flame appears to be in the pre-activation zone of the two systems. Hydrogen is far more readily generated from propane than from methane, which suggests that the H_2-concentration in the pre-activation zone of a propane flame is high and OH and O diffusing into the zone disappear rapidly in reactions with H_2, to form H. In the methane system the H_2-concentration is presumably low and the dominant chain carriers in the pre-activation zone are OH and O rather than H. One may then interpret

the data to signify that CH_3Br and CF_3Br are about equally efficient with respect to destruction of OH and O, but that H-atoms are more efficiently destroyed by CH_3Br than by CF_3Br. This interpretation is speculative at present inasmuch as there is no independent evidence available for the assumption that CF_3Br reacts less readily with H than CH_3Br.

Experimental Methods

The purpose of this task was to provide a relative ranking of various candidate flame inhibiting agents on the basis of their ability to reduce the flame strength of a diffusion flame. The opposed jet burner, similar to that used by Friedman and Levy (ref. 3), was used for this purpose.

Butane was selected originally as the experimental fuel because it approximates the properties of the heavier hydrocarbons encountered in fuel fires. However, its low vapor pressure (13 psig) at room temperature creates difficulties in metering and the high stoichiometric ratio with air (1:31) causes problems in burner operation. The use of an inert gas diluent relieves some of these problems but introduces others. Consequently, a change was made to propane as the fuel in the experiments described here.

The agents studied in the program fell in two groups; agents previously studied which were used to check the performance of the burner, and candidate agents for encapsulation suggested by Ames Research Center. The first group included CH_3Br, CF_3Br, and CCl_4. The second group included CBr_4, $CHBr_2CHBr_2$, CCl_3Br, CF_2BrCF_2Br, ICl_3, SO_2, H_2O, $CF_2ClCFCl_2$, tris (2,3 dibromopropyl) phosphate, and molybdenum carbonyl. Difficulties in encapsulating ICl_3 caused it to be dropped from the program, and $CHBr_3$ was substituted in its place. The low vapor pressure of tris (2,3 dibromopropyl) phosphate prevented effective evaluation. Molybdenum hexacarbonyl was received too late in the program for detailed study.

Apparatus. - The burner, shown in figure 4, consisted of opposed coaxial vertical stainless steel tubes, 0.46 cm i. d. and with a 1.0 cm separation between tube ends. The flame was shielded from drafts with a Pyrex sleeve or in later experiments, with a metal sleeve having an easily replaceable Pyrex window consisting of a microscope slide. Frequent replacement of the slide was necessary because of carbon or other solid deposition during experiments.

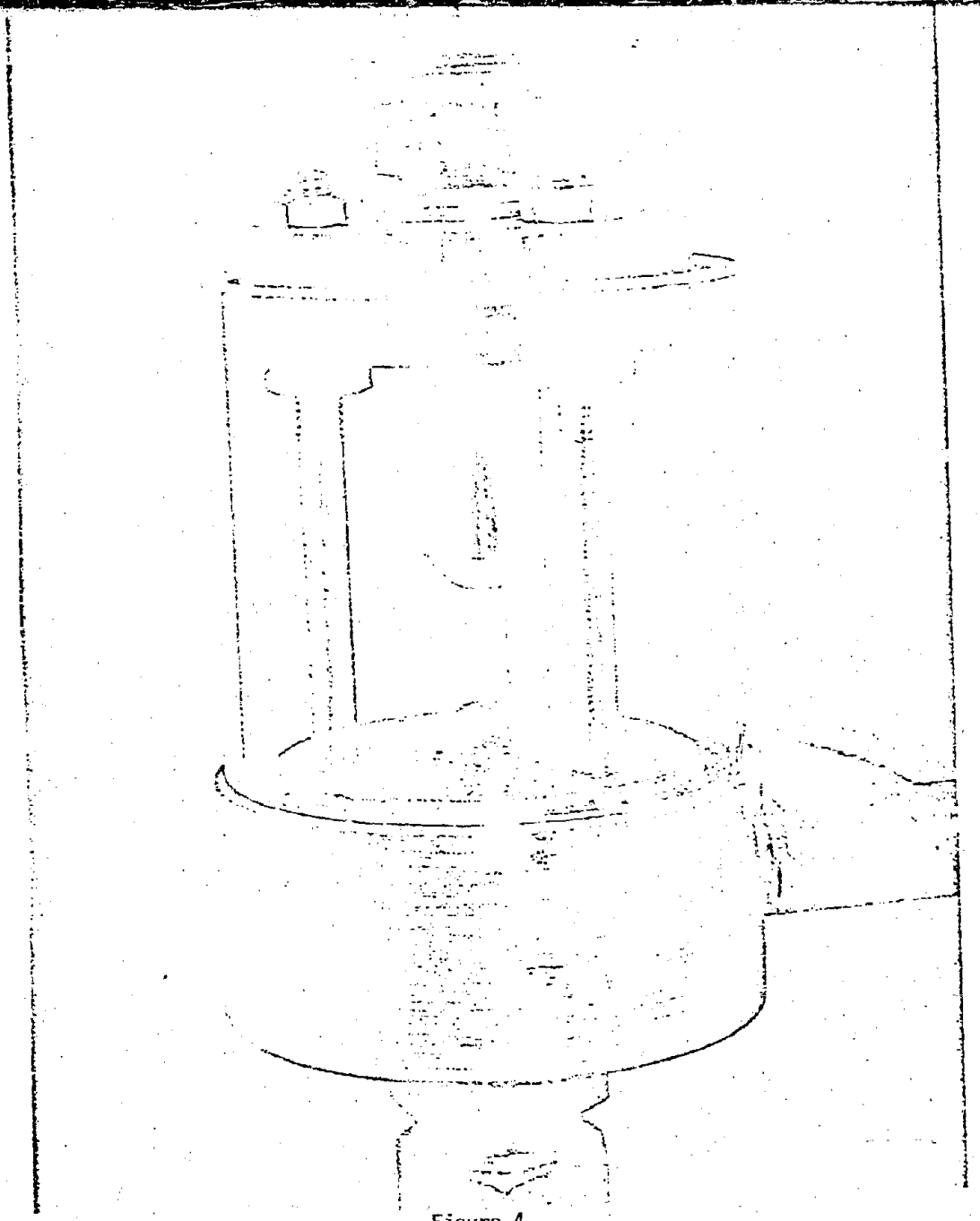

Figure 4
Opposed Jet Burner

Each burner tube was jacketed with an outer concentric tube for temperature control. Heat exchangers consisting of jacketed 4 ft. spirals of 1/2 in. copper tubing were installed in the gas lines immediately before the burner. Circulation of oil from a constant temperature bath through the burner and heat exchangers allowed the temperature of the gases entering the burner chamber to be kept at any desired value between room temperature and 220°C. Burner temperatures were selected to prevent condensation of inhibitor in the lines.

Air and propane were metered to the burner through critical orifices used with precision pressure regulators and bourdon gauges (ref. 15). The orifices were calibrated with a wet test meter. Figure 5 shows a general view of the apparatus before installation of thermal insulation.

Three methods were used for metering the inhibitor. Gaseous agents, CH_3Br, CF_3Br, and SO_2 were metered through critical orifices similar to those used for propane and air. Low boiling liquids were metered from a heated reservoir at superatmospheric pressures through calibrated orifices. Concentrations were checked after each burner run by trapping a sample of the propane-agent mixture, freezing out the agent with dry ice, pumping off the propane, warming to room temperature, and measuring the residual vapor pressure of agent. High boiling liquids were metered with a motor driven syringe. Various syringe sizes and drive rates permitted a wide range of feed rates. The syringes could be heated to permit their use with low melting solids. Calibration with various syringe and drive speed combinations was accomplished gravimetrically using mercury. The liquid was injected directly onto the heating element of an evaporator which could be inserted into either the fuel or air line by a system of valves. The temperature of the heating element, which consisted of an asbestos cloth wick woven with nichrome heating wire, was controlled manually by a variable transformer and monitored by a chromel-alumel thermocouple.

Operating Procedure. - A typical measurement is made in the following manner. The burner temperature control system is brought to the desired temperature selected on the basis of the physical properties of the agent to be evaluated. Fuel and air flows are started to the burner. The flame

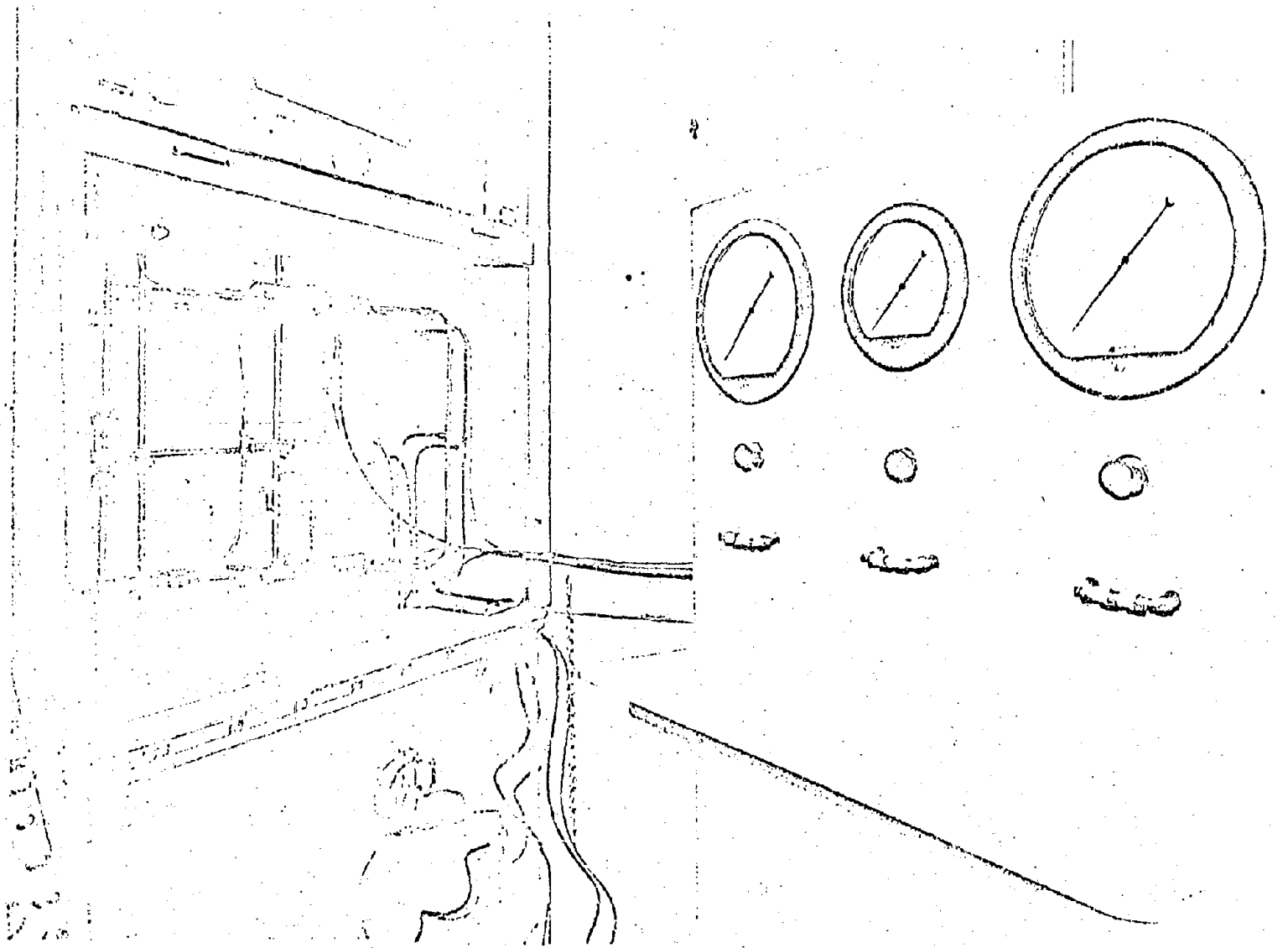

Figure 5
Burner and Controls

is ignited by a bunsen burner and the flow rates of both fuel and air are adjusted until the flame stabilizes. The flame is then centered between the jets by adjusting either the air or fuel flow while observing the flame through a cathetometer. The flow rates are then increased in small increments, maintaining the flame at the midpoint between the jets, until a faint hole appears in the center. This is recorded as the hole point and is verified twice, (1) by increasing the flow rates beyond the minimum hole opening, thereby increasing the size of the hole, and then returning to the minimum opening from this direction and (2) by decreasing the flow rates to a point where no hole is visible and finding the minimum critical flow again by increasing the flows. The flow of fuel at the minimum rate at which a hole exists is the value reported as the "critical fuel flow without agent." The agent is then introduced into the fuel by bypassing the fuel through the agent injection system after first reducing the flow of both gases below the hole point. The procedure used in determining the hole point without agent is repeated. This new value for the fuel flow is recorded as the "critical fuel flow with agent." Figures 6A and 6B are photographs of the flame before and after reaching the critical flow conditions. The flow was increased well beyond the critical value in figure 6B to increase the hole size for photographic purposes.

The detection of the critical point by this procedure requires subjective judgment on the part of the operator. An experienced operator will usually detect the hole point at a slightly lower flow than an inexperienced one. However, since only relative flow rates are used in calculating inhibitor efficiencies, no serious error results if all of the data on a given inhibitor are taken by the same operator. In practice, two experienced operators obtained all of the data used for inhibitor evaluation. An instrumental method of detecting the hole point would be a desirable improvement in the apparatus. The critical fuel flow without inhibitor varied from day to day for unknown reasons. A base point at zero inhibitor concentration was determined at the start of each day's run and redetermined at intervals during the day.

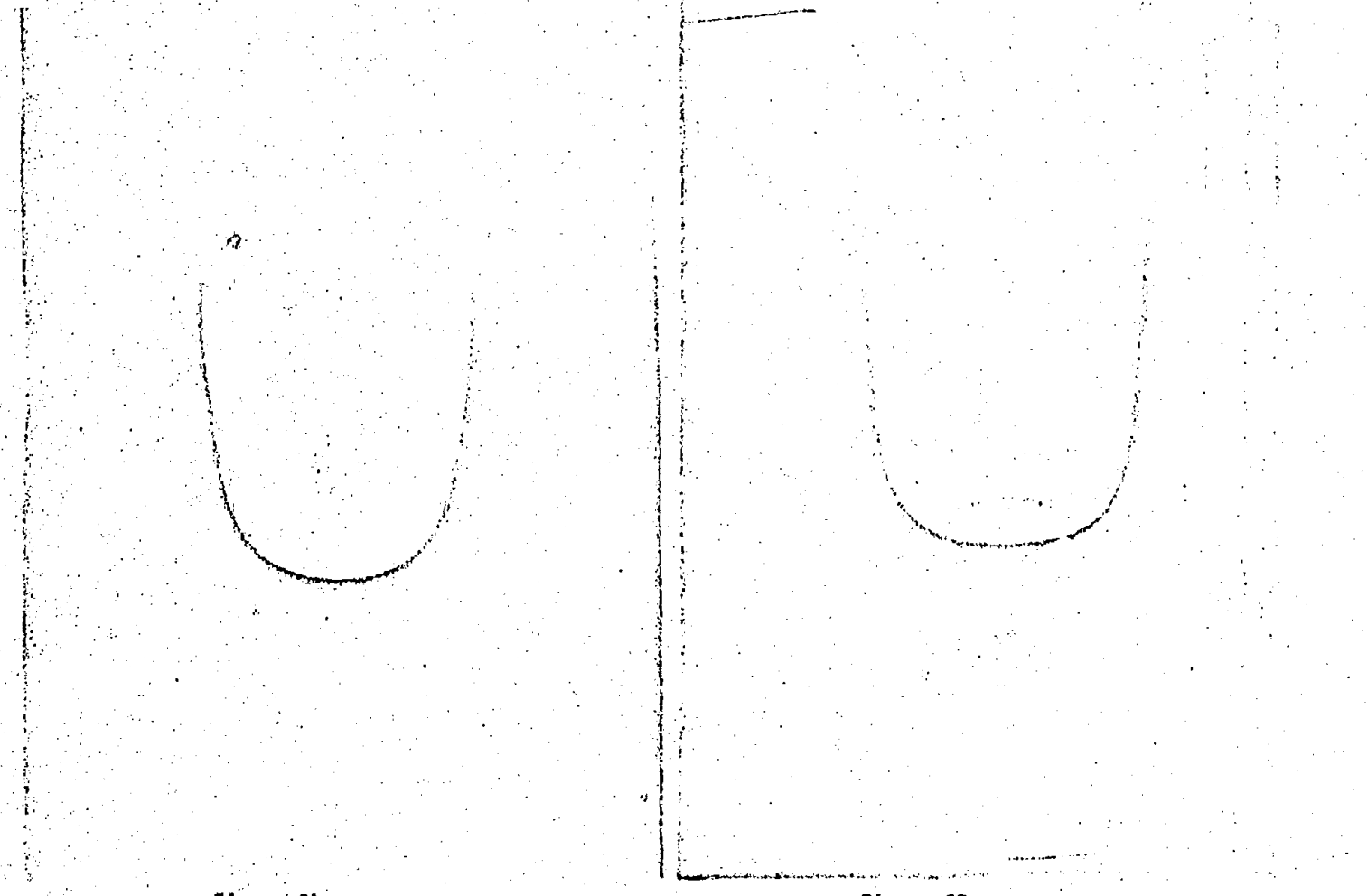

Figure 6A
Figure 6B
Burner Flame Before and After Reaching Critical Flow Conditions

AGENT RELEASE FROM MICROCAPSULES

The extinguishing agents studied in this program are intended for use in the form of polymer coated microcapsules. These are to be incorporated into a polymeric matrix or foam which can be used for structural or insulating purposes. In the event of a fire the agent will be released, extinguishing the fire. It is necessary that the microcapsules be sufficiently stable that the agent is not lost during long exposure to ambient conditions. At the same time it must be released readily into the vapor phase under fire conditions. An understanding of the way in which the agent escapes from the capsules under various conditions will be useful in guiding the development of practical systems. A variety of experiments were performed to contribute to this understanding.

Microencapsulated extinguishing agents were prepared and furnished by the National Cash Register Company using encapsulation procedures developed in their laboratories. Briefly, the agent is suspended, in the form of small droplets (or solid particles), in an immiscible liquid containing a dissolved polymer. The polymer is caused to precipitate on the surface of the droplet. Various treatments may then be used to insolubilize the polymer coating and remove the carrier liquid. Properties of encapsulated agents supplied for use on this program, as reported by NCR, are summarized in Table AII of the Appendix.

Gelatin and polyvinyl alcohol (PVA) were the principal wall materials used. In some cases a phenolic resin was added to insolubilize and harden the wall and reduce agent permeation. The agent content of microcapsules ranged from 67 to 97 percent and particle sizes were in the 50-300 micron range.

Physical Examination. - Photomicrographs of encapsulated $CF_2ClCFCl_2$ are shown in figures 7A and 7B. The spread of particle size is typical of most of the samples examined. The protrusions at opposite ends of the spheres are reported to be due to peculiarities in the encapsulation process. They were much less prominent or almost entirely absent in some samples.

Detailed particle size distribution curves have been reported by NCR. Samples were screened in our laboratory by standard techniques to provide

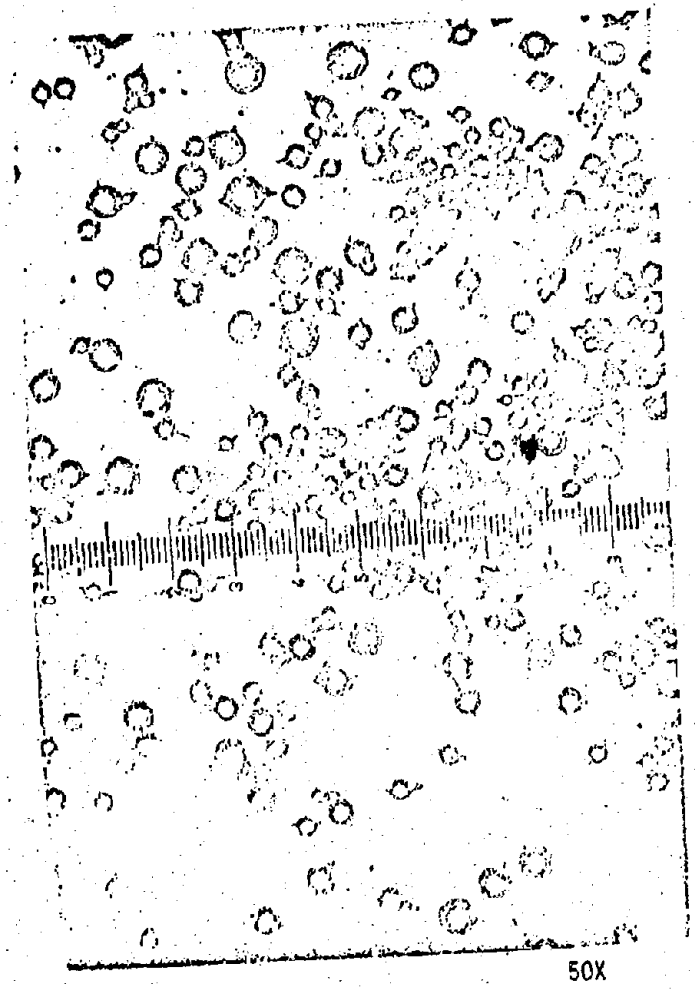

Figure 7A

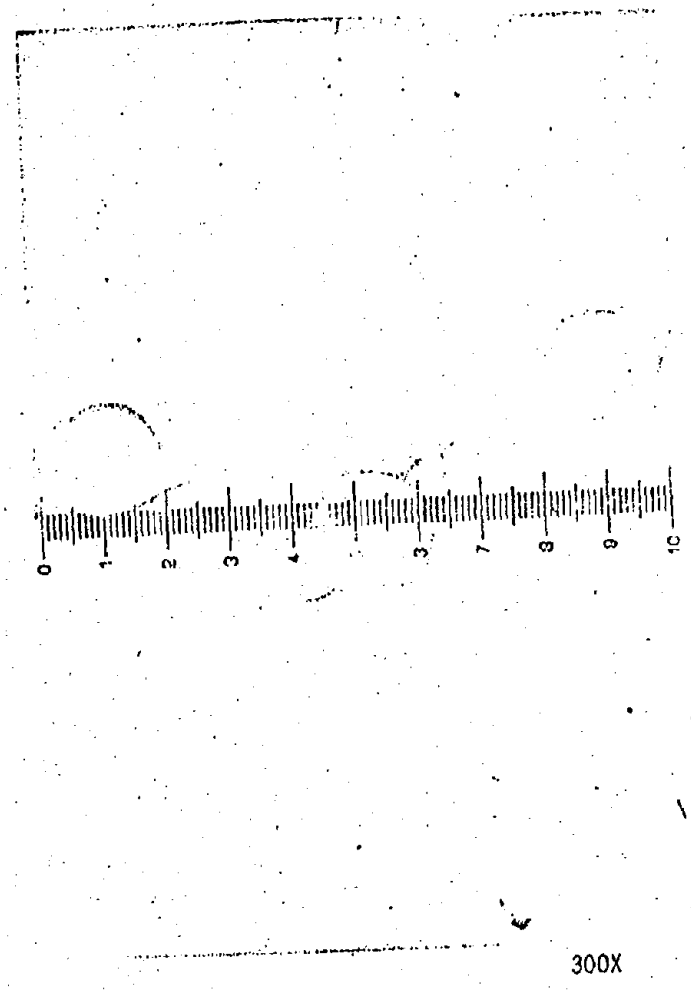

Figure 7B

Figure 7A
Photomicrographs of $CF_2ClCClF_2$ Encapsulated in Gelatin

samples with narrow size distribution for further experiments. Typical results are shown below.

Sample No. S-61068-1

Agent:	Trichlorobromomethane
Encapsulant:	Polyvinyl alcohol

Particle Size Analysis:

Size (μ)	Weight Percent
>88	44.50
62 to 88	47.30
53 to 62	2.60
<53	5.95

Sample No. S-71568-1

Agent:	Tris (2,3-dibromopropyl) phosphate
Encapsulant:	Polyvinyl alcohol

Particle Size Analysis:

Size (μ)	Weight Percent
>125	37.60
88 to 125	5.64
62 to 88	56.40
53 to 62	0.35
< 53	0.00

Sample No. S-61168-2

Agent:	Carbon Tetrabromide
Encapsulant:	Gelatin

Particle Size Analysis:

Size (μ)	Weight Percent
>125 50.0	50.00
88 to 125	44.60
62 to 88	5.36
53 to 62	0.01
< 53	0.01

An average wall thickness can be estimated from the percent of wall material, assuming spherical capsules with uniform walls. Values in the range of 2-20μ are calculated in this way. Obviously the assumption of spherical symmetry is poor for a sample such as that shown in figure 7. Microcapsules were embedded in paraffin and sectioned with a microtome. Microscopic examination showed wide variations in wall thickness, as shown in the sketch in figure 8. The method of preparation suggests that the average wall thickness should be relatively uniform within a batch, regardless of particle size. Preliminary examination appears to support this assumption. The smaller particles must then have a much smaller agent to wall weight ratio than the larger particles.

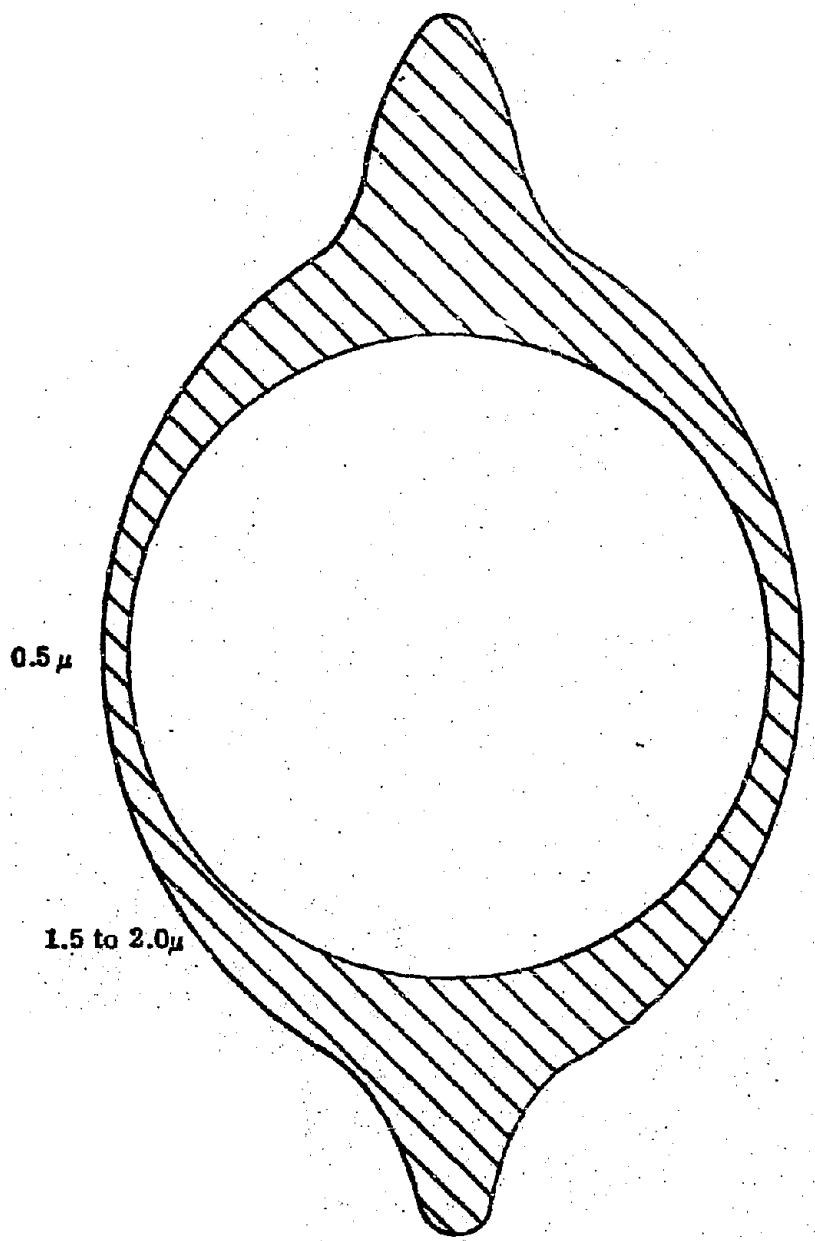

Figure 8
Sketch of Typical Capsule Cross Section
$CF_2ClCFCl_2$ in Gelatin

Vapor release rates at ambient temperature. - Many of the extinguishing agents studied have appreciable vapor pressures at normal operating temperatures. Encapsulation reduces the rate of evaporation, but it is necessary to know whether the rate of agent loss is sufficiently slow to permit use of the encapsulated agents under conditions of long exposure. Permeability measurements at atmospheric pressure and 20 or 60°C for a number of samples were reported by NCR. Similar measurements were made under vacuum (<1 torr) in this laboratory. Samples were spread in an aluminum weighing dish in a layer one capsule deep and placed in a vacuum desiccator, from which, at selected time intervals, the dish was removed and weighed. Typical results are given in Table IV. Where available, comparable data at atmoshperic pressure from NCR have been included for comparison.

The low volatility of $CF_2ClCFCl_2$ (boiling point 47.6°C, vapor pressure at 25°C 335 torr) shows the effectiveness of the encapsulation technique. The small loss from the trichlorobromomethane and tris (2,3-dibromopropyl) phosphate is probably due to loss of residual solvent or water from the surface or capsule wall since the weight quickly levels off at a nearly constant value. The phosphate will have a very low vapor pressure at 25°C (vapor pressure 4 torr at 250°C), but $CBrCl_3$ (boiling point 104°C) will have a significant vapor pressure at 25°C. The greater weight loss from the smaller particle size fractions, which have a greater surface area and larger percent of wall material, supports this view.

Carbon tetrabromide, on the other hand, exhibits an entirely different type of behavior. Despite its low vapor pressure (boiling point 189.5°C) it diffuses readily through the capsule wall and is almost completely lost within 24 hours. Carbon tetraiodide apparently exhibits similar behavior. The sample received showed evidence of agent migration and instability on storage in a sealed container.

Vapor release at elevated temperatures. Single particle experiments. A number of experiments were carried out in an effort to observe the behavior of single microcapsules on rapid heating. Capsules were placed on an electrically heated nichrome ribbon and observed under a low power microscope. On heating the ribbon the capsules were observed to explode like popcorn,

Table IV

Vacuum Weight Loss from Microcapsules
25°C, ≈ 1 torr

Sample No. Unassigned
Agent: $CF_2ClCFCl_2$
Encapsulant: Gelatin

Time (hr)	Wt. Loss (%)
1	0
2	0
4	0
7	0
24	.045

Sample No. S-61168-1

Agent: Trichlorobromomethane
Encapsulant: Gelatin

% Agent : 87

	Weight Loss (%)				
Time (hr.)	As Received	>88μ	62 to 88μ	<53μ	NCR (1 atm)
1	1.09	1.30	1.35	1.05	
2	1.25	-	-	-	
4	1.42	1.08	1.51	1.02	
7	1.42	1.39	1.64	1.25	
24	1.41	1.61	1.73	1.16	0

Sample No. S-61168-2

Agent: Carbon Tetrabromide
Encapsulant: Gelatin

% Agent: 81

	Weight Loss (%)		
Time (hr.)	>125μ	88 to 125μ	NCR (1 atm)
1	22.2	10.8	
2	45.4	23.7	
4	46.6	36.7	
7	68.4	44.1	
24	78.3	56.2	19

Table IV (Concluded)

Sample No. J-61068-1

Agent: Trichlorobromomethane
Encapsulant: Polyvinyl alcohol

% Agent: 96

Time (hr.)	Weight Loss (%) As Received	>88μ	62 to 88μ	<53μ	NCB (1 atm)
1	0.298	0.420	0.511	0.522	
2	0.357	0.640	0.320	0.820	
4	0.502	0.706	0.695	0.940	
7	0.590	0.825	0.838	1.52	
24	0.935	1.44	1.24	3.02	4

Sample No. S-71568-1

Agent: Tris (2,3-dibromopropyl) phosphate
Encapsulant: Polyvinyl alcohol

Time (hr.)	Weight Loss (%) As Received	>125μ	62 to 88μ
1	0.476	-	-
2	0.574	0.454	0.434
4	0.615	0.350	0.437
7	0.650	0.493	0.476
24	0.680	0.410	0.486

Sample No. D-71268-1

Agent: Tris (2,3-dibromopropyl) phosphate
Encapsulant: Gelatin

Time (hr.)	Weight Loss (%) As Received	>88μ	62 to 88μ
1	5.70	2.19	3.14
2	6.50	2.36	3.92
4	6.65	2.28	3.82
7	6.88	2.30	4.00
24	6.95	2.40	4.12

scattering the capsules out of the field of view. Attempts to take high speed motion pictures for study failed because of insufficient magnification and illumination with the equipment available. Attempts to levitate the capsules in a hot air stream also failed because the irregularly shaped particles could not be kept within the field of view at adequate magnification. Capsules were suspended in oil and observed on the hot stage of the microscope. Hairline cracks appeared just before the capsules burst and left the field of view. Possible softening effects of the oil on the capsule wall discouraged further work with this technique.

A technique was developed for mounting individual microcapsules on the head of a one mil chromel-alumel thermocouple or on a fine glass fiber adjacent to the thermocouple. The capsule was placed in a stream of nitrogen issuing from an electrically heated heat exchanger and observed with a stereo microscope. The thermocouple temperature was recorded on a strip chart and a shorting switch enabled the operator to record the time of significant events. The heating rate was approximately 20°C/min and the gas velocity was about 5 cm/sec. The results of observation of a number of capsules by this method are reported in the following table.

The more volatile agents, $C_2F_3Cl_3$ and $C_2F_4Br_2$, show fairly consistent behavior; rupturing at an average temperature of 130°C, well above the boiling points (47°C in each case). The vapor pressure at this temperature would be approximately 100 psig, although the temperature of the capsule may lag behind that of the thermocouple. Swelling of the capsules prior to rupture was observed in many cases. Variations in cell wall thickness undoubtedly account for much of the observed variations in behavior.

The less volatile tris (2,3 dibromopropyl) phosphate survives to a much higher temperature, indicating that vapor pressure rather than thermal degradation of the wall material is the primary cause of wall failure. Softening points of the gelatin and PVA wall materials, as observed on the hot stage, were 168°C and 208°C respectively. The actual capsule walls which are treated with hardening agents would be expected to soften at somewhat higher temperatures. The capsule swelling observed at high temperatures may indicate thermal decomposition of the agent.

Table V

Observations of Single Microcapsules
Heated in a Nitrogen Stream

Sample No.	Agent	Wall Material	Sphere Size μ	Rupture Temp. °C	Comments
Unknown	$C_2F_3Cl_3$	Gelatin	63	103	
			89	-	Agent lost without rupture
			114	149	
			117	141	
			101	137	
			114	126	
			114	134	
			120	126	
			203	-	Agent lost without rupture
J-61068-1	CCl_3Br	PVA	89	-	No observable change
			89	-	Walls darkened, no rupture
			76	-	Walls darkened, no rupture
			132	177	
			90	180	
S-61168-1	CCl_3Br	Gelatin	101-204	-	Six experiments performed, all lost agent without rupture between 100 and 200°C.
S-61168-2	CBr_4	Gelatin	85	133	
			90	150	
			241	93	
			114	222	
J-80168-1	CBr_4	Gelatin	254	57	
			190	225	
			190	155	
			89	61	
			190	77	
J-80868-1	CBr_4	PVA	89	184	
			89	-	Lost agent, no rupture
			76	175	
			76	-	No change up to 307°C
			64	96	
			76	-	Wall darkened, no rupture

Table V - Concluded

Observations of Single Microcapsules
Heated in a Nitrogen Stream

Sample No.	Agent	Wall Material	Sphere Size μ	Rupture Temp. °C	Comments
S-71568-1	Tris (2,3-dibromo-propyl) phosphate	PVA	89	231	
			89	173	
			76	194	
			64	122	
			65	342	
			75	347	
			50	347	
D-71268-1	Tris (2,3-dibromo-propyl) phosphate	Gelatin	114	212	
			127	-	Sphere grew to 165 μ. no rupture
			101	282	
J-72968-1	$C_2F_4Br_2$	PVA	152	-	Agent lost, no rupture
			102	133	
			166	143	Sphere grew to 170μ
			165	115	Sphere grew to 182μ
			139	117	Sphere grew
D-80268-1	P-nitro aniline bisulfate	Parlon	254	126	Walls melting
			250	114	Walls melting

The behavior of CCl_3Br and CBr_4 was even more erratic. It appears that these agents diffuse through the cell walls readily at elevated temperatures, as also observed at room temperature. Depending on the rate of heating and wall conditions, a critical pressure may or may not be reached before agent is lost by diffusion. Thermal decomposition of the agent and reaction of the products (Br_2) with the wall material may further complicate the picture.

Isothermal release of agent at elevated temperatures. - Samples of encapsulated agent were heated isothermally and weight loss with time was continuously monitored. These experiments were carried out by placing agent (~1 gram) in a light weight aluminum capsule which in turn was set on the pan of a sensitive balance. The balance was of the type that had a single pan mounted on top of the cabinet. A thermocouple was positioned in the sample bed and a preheated oven was lowered around the capsule.

Typical results are plotted in figures 9, 10, 11, and 12. After an initial rapid weight loss whose magnitude increases with temperature, the rate of agent loss decreases to a low and nearly constant rate relatively independent of temperature. The experiment was performed by placing a preheated furnace over the sample container at zero time. Temperature equilibrium was established in approximately one to two minutes, much less than the transient weight loss period observed at the start of the experiment. It appears that a portion of the agent is released more readily than the remainder. A small portion of this weight loss may represent surface moisture, or solvent or agent dissolved in the outer layers of the cell wall. The bulk of readily released agent, however, must come from the interior of the capsules. A "popping" noise could be heard in the container during the period of rapid weight loss, diminishing with time. Microscopic examination of the capsules after the end of the heating period showed a portion of them to be empty while the remainder were partially filled with agent.

The results suggest a considerable degree of heterogeniety in capsule structure with variations in size, wall thickness, and perhaps even in porosity of the wall. On heating, pressure will increase inside the capsule, even for materials of low vapor pressure, since the coefficient of expansion of the agent will be greater than that of the wall. Weak or thin-walled capsules will rupture and release all of their agent content. The larger capsules would be expected to rupture more easily (figure 10). After release of the agent from these more fragile capsules, further agent loss is apparently due to a slow diffusion process with a low energy of activation. The polyvinyl alcohol capsules have much greater wall strength than the gelatin capsules (figure 11).

Carbon tetrabromide shows an entirely different type of behavior (figure 12). The agent diffuses readily through the cell wall. Because of the low vapor pressure, no significant pressure increase occurs and no capsule rupture is observed.

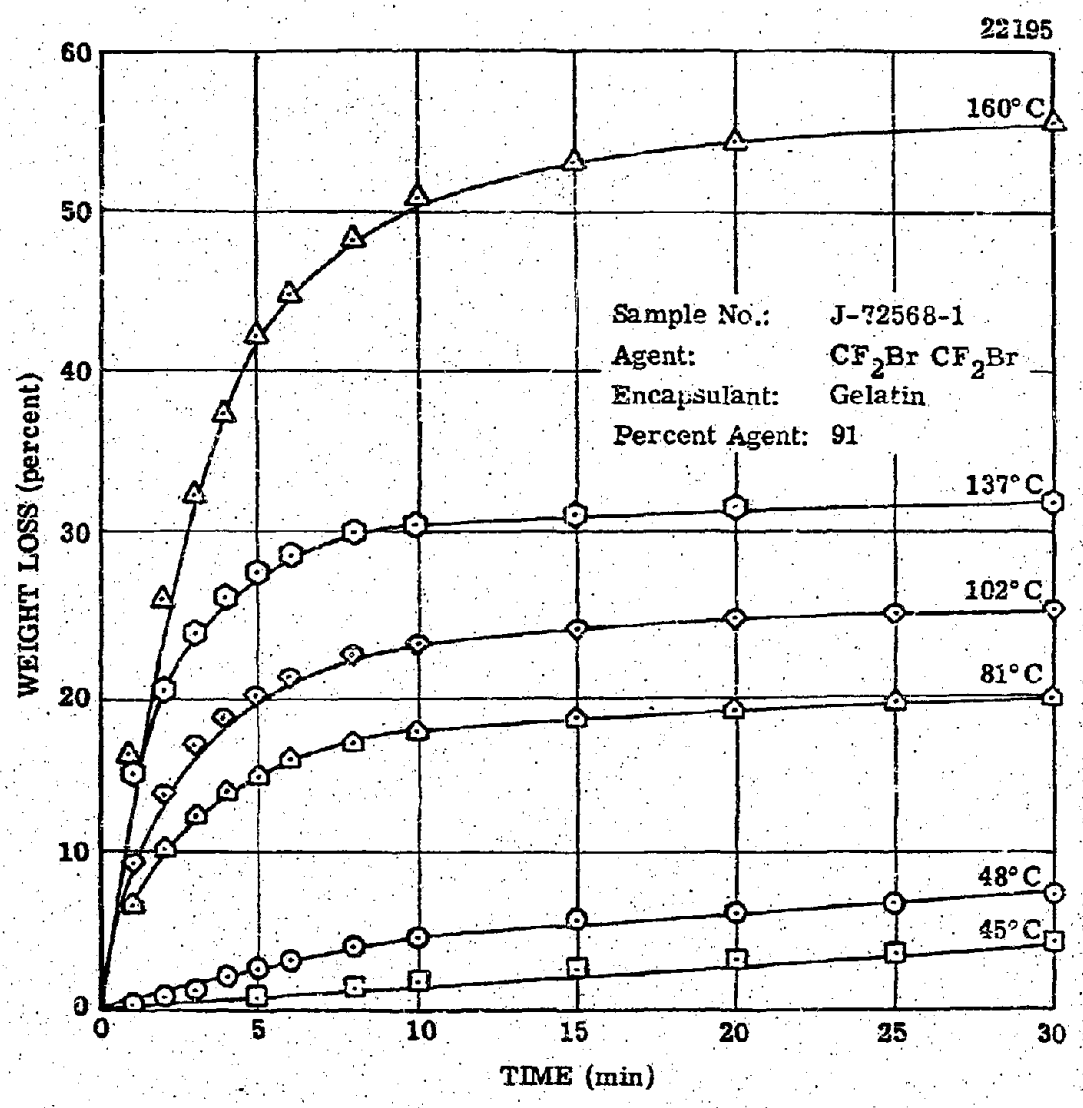

Figure 9. Isothermal Release of Agent.

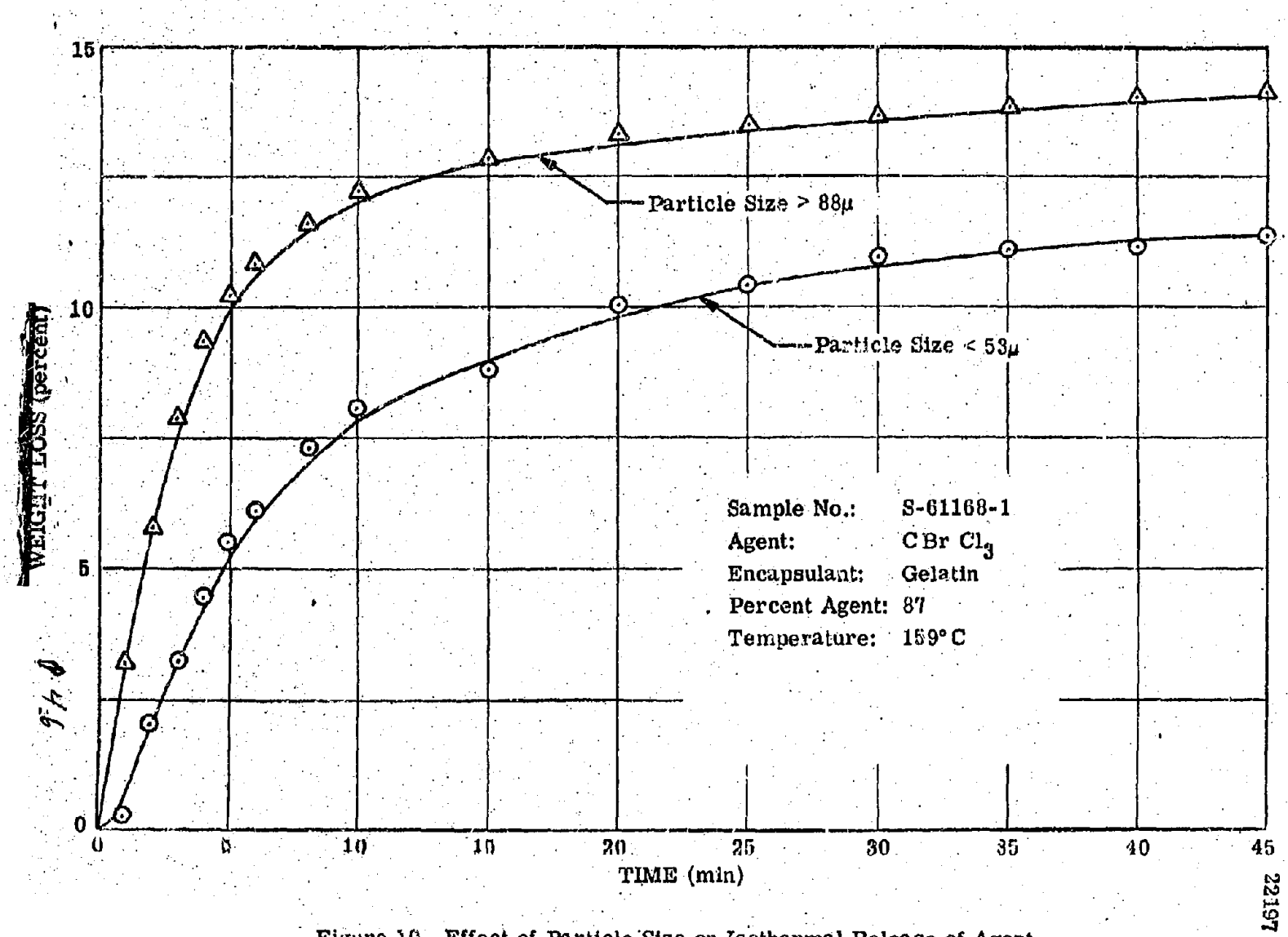

Figure 10. Effect of Particle Size on Isothermal Release of Agent.

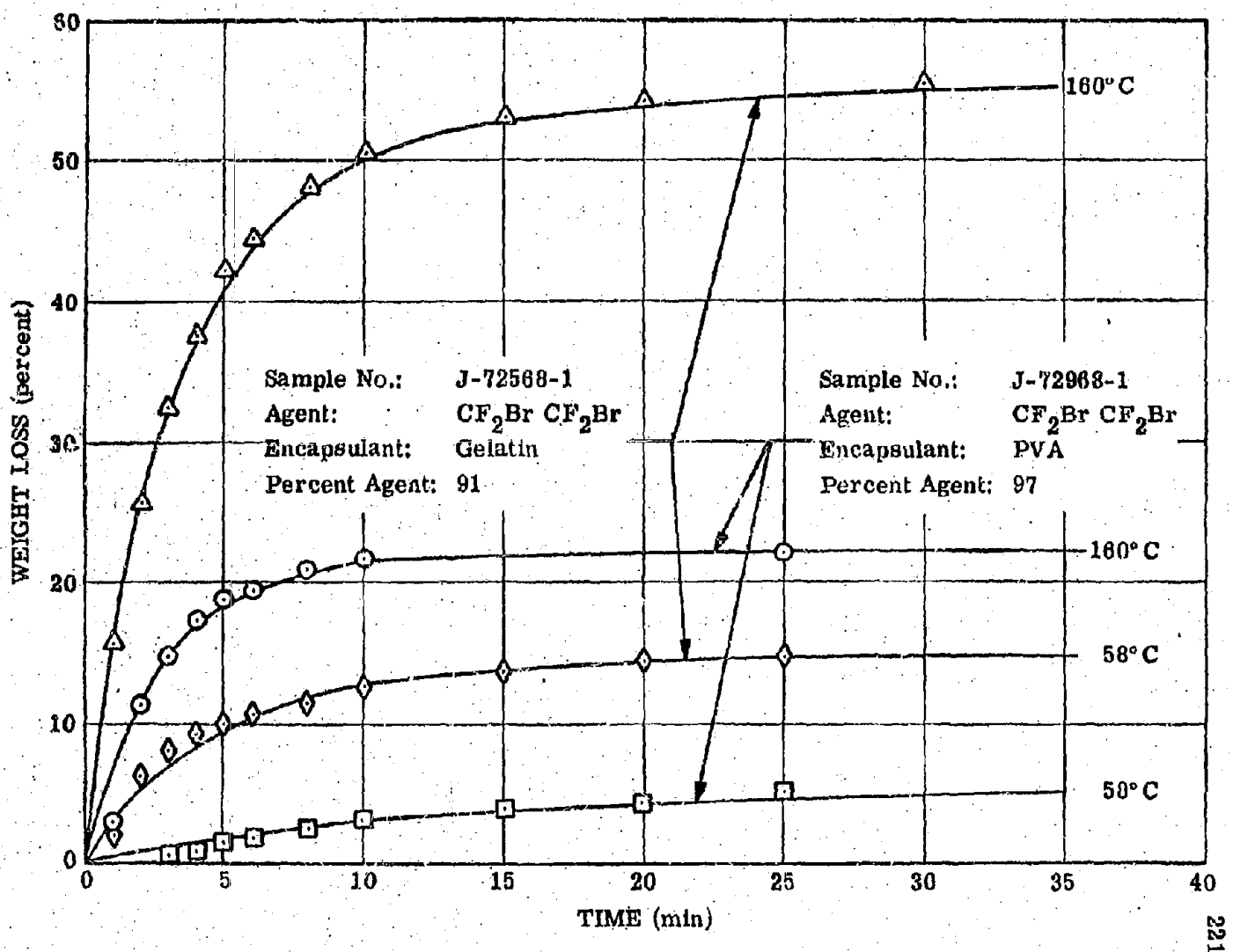

Figure 11. Effect of Encapsulant on Isothermal Release of Agent.

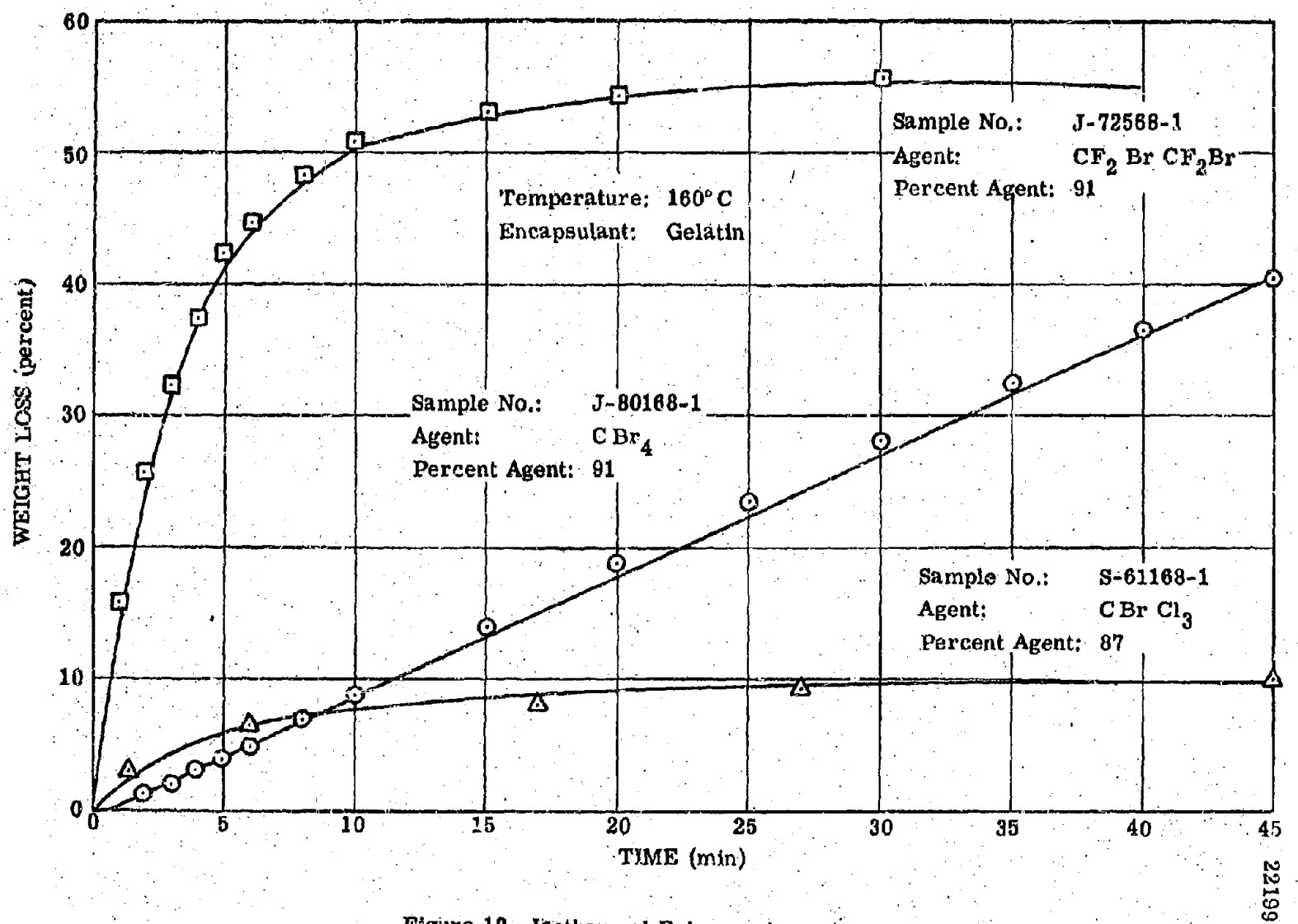

Figure 12. Isothermal Release of Different Agents.

Agent release on rapid heating of microcapsules. - An apparatus was designed for the rapid heating of small samples of encapsulated agents. The apparatus consisted of a stainless steel tube, 0.375 in. o. d. by 0.314 in. i. d. by 2.0 in. long. The total free volume of the system was 2.15 cc. The lower end of the tube was closed by a welded plate while the upper end was fitted with a "T" fitting which provided ports for a thermocouple and a Kistler Model 601 pressure transducer. The outputs of the thermocouple and pressure transducer were fed to a dual channel oscilloscope fitted with a Polaroid camera. The thermocouple could be positioned either in contact with the interior of the chamber wall or in the gas phase.

In performing an experiment, the chamber was loaded with a small weighed sample of encapsulated agent (≈0.1 gm) and placed in a preheated tube furnace. Rates of temperature rise inside the chamber of about 30°C/sec were typical. Representative pressure vs. time and temperature vs. time records obtained from the oscilloscope are shown in figures 13 through 16. The records are reduced to standard units (figure 17) and cross-plotted to give pressure vs. temperature curves (figure 18).

Figures 17 and 18 show a detailed analysis of the data from figure 13. This shows the release of agent from a sample of CCl_3Br encapsulated in gelatin. The chamber pressure follows the vapor pressure curve for the agent during the initial part of the experiment, but lags behind at the higher temperatures, showing the retarding effect of the capsules on the rate of agent release. The maximum pressure agrees well with the calculated value, indicating the lack of significant pyrolysis of the wall material at these temperatures. Examination of the residue in the chamber at the end of an experiment showed the capsule shells to be empty but intact.

Figure 14 shows a similar experiment with CBr_4 encapsulated in gelatin. A slight drop in pressure with an increase in temperature is observed at one point, indicating the cooling by evaporating caused by the sudden release of liquid agent into the superheated gas. In figure 15 unencapsulated CBr_4 was placed in the chamber. The temperature remains approximately constant at the boiling point of CBr_4, increasing slowly with pressure until all of the

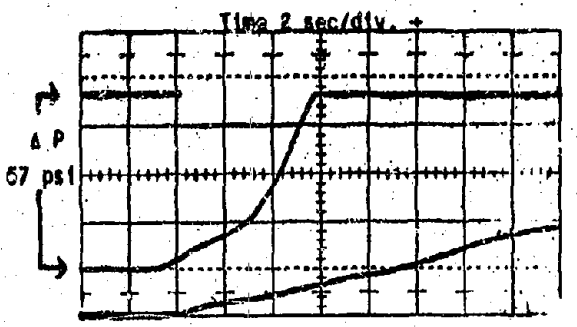

Figure 13
CCl_3Br in Gelatin

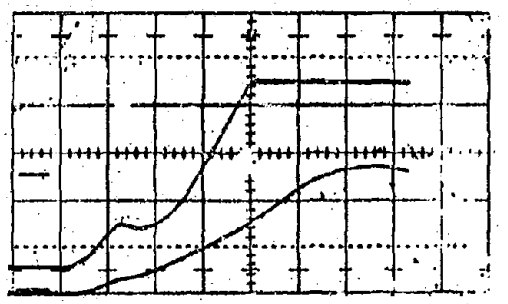

Figure 14
CBr_4 in Gelatin

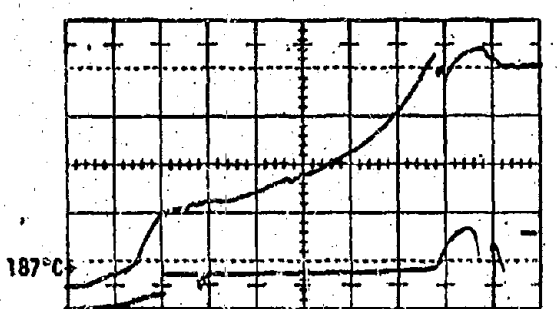

Figure 15
CBr_4

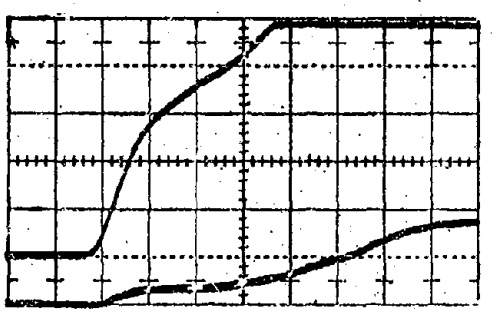

Figure 16
Tris (dibromopropyl) phosphate in PVA

Typical Pressure/Time and Temperature/Time Records
From Rapidly Heated Microcapsules

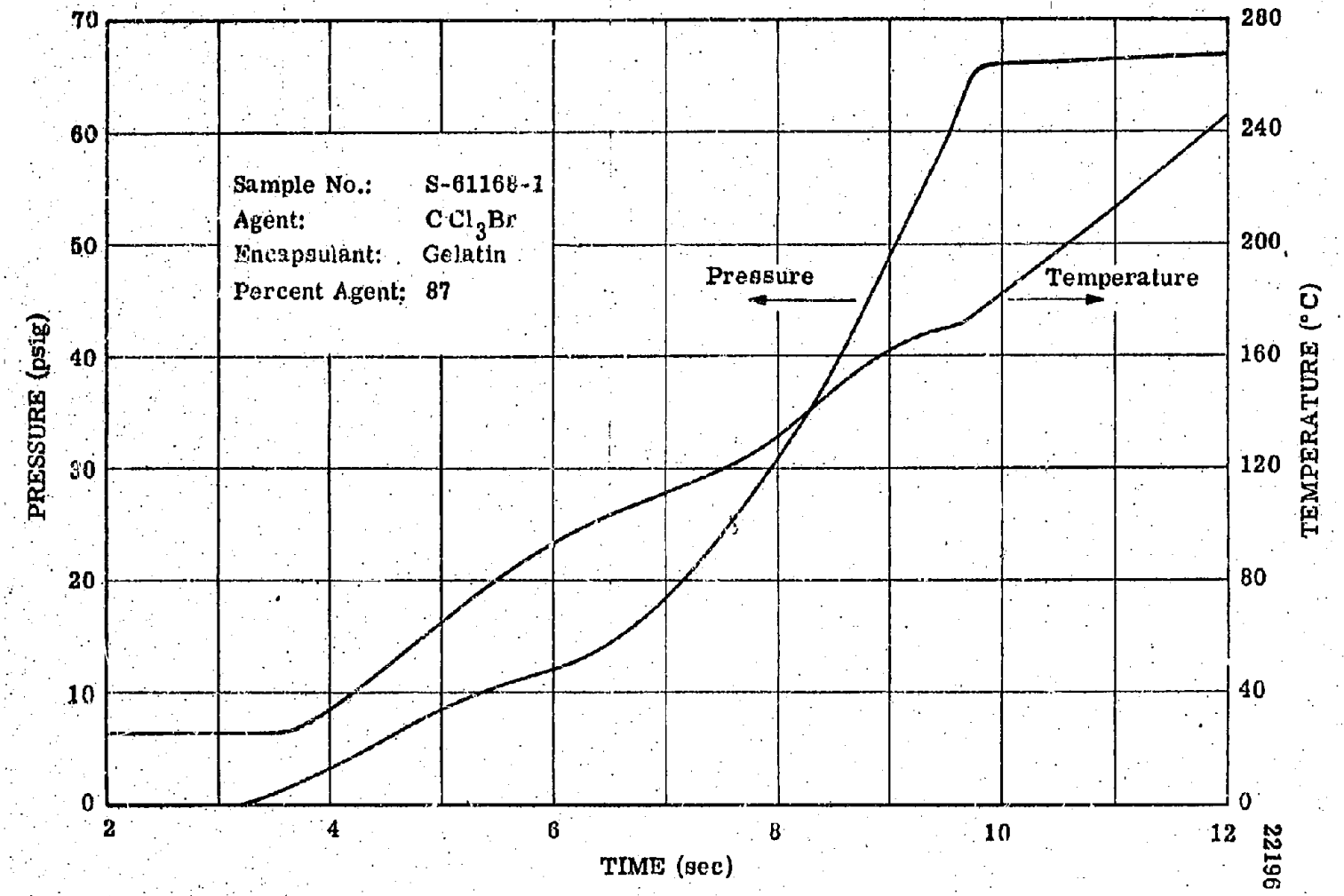

Figure 17. Rate of Pressure and Temperature Increase (From Figure 13).

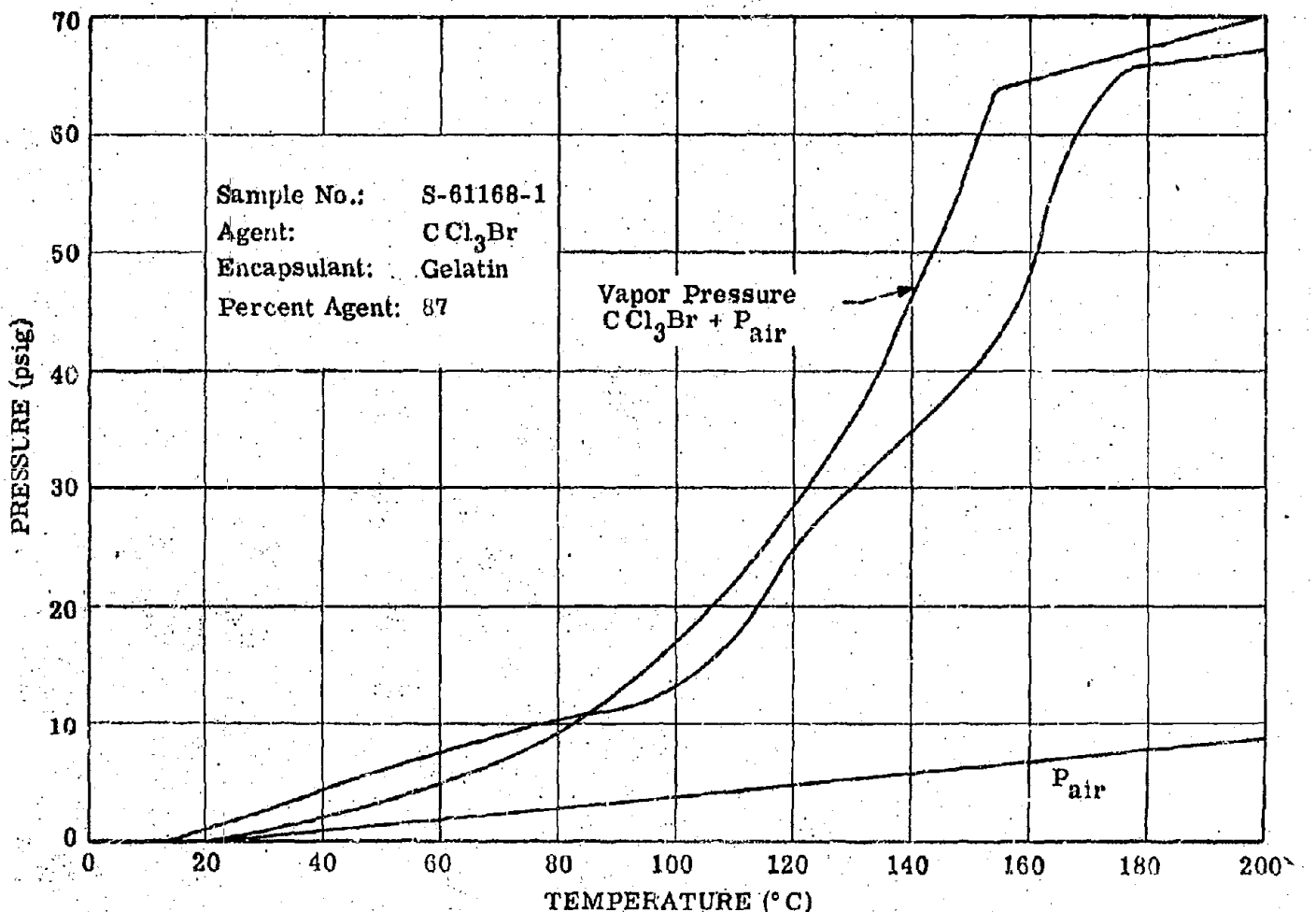
Sample No.: S-61168-1
Agent: CCl_3Br
Encapsulant: Gelatin
Percent Agent: 87
Vapor Pressure
$CCl_3Br + P_{air}$
P_{air}
PRESSURE (psig)
TEMPERATURE (°C)
0
10
20
30
40
50
60
70
0
20
40
60
80
100
120
140
160
180
200

agent has vaporized. Figure 16 shows an experiment with tris (2,3-dibromopropyl) phosphate encapsulated in PVA. Here evidence of rapid vaporization is absent but thermal decomposition of the agent is occurring since the chamber pressure greatly exceeds the calculated vapor pressure.

Difficulties in defining heat transfer conditions in this apparatus discouraged attempts at a more quantitative analysis of the results.

Discussion of Vapor Release Mechanisms

Two situations can be cited where the nature of the release of fire extinguishing agents from microcapsules is important. The first involves storage under ambient conditions, either of the unmodified capsules or of the capsules embedded in a polymeric matrix for structural applications. Loss of agents under these conditions will be undesirable because of loss of fire extinguishing capacity and because of undesirable properties of the released agent, such as toxicity or corrosive action. Agent loss at ambient temperatures will be controlled by permeation processes. The second situation involves actual fire conditions where the microcapsules will be subjected to an intense heat flux. The internal pressure in the capsule will increase while the capsule wall is weakened. Capsule rupture will be the principal mode of agent release under these conditions. The experiments described in the preceeding section provide support for these separate mechanisms of agent release.

The problem of vapor release under storage conditions is essentially that of permeation of a fluid through a membrane. This can occur through pores or cracks in the membrane, in which case the process is basically one of flow through an orifice or capillary. Or it may occur by a true diffusion process, sometimes called activated diffusion. In the latter mode the fluid dissolves in the membrane material, diffuses through it, and is released on the other side. This is believed to be the method by which CBr_4 escapes from gelatin capsules (figure 12), and it also applies to the very slow release of agent shown in figures 9-12 after the initial rapid release period. There are a number of influence parameters -- temperature, pressure,

wall material, wall thickness and agent volatility -- which have been investigated experimentally and the following simplified analysis (ref. 16) provides a basis for understanding some of the observed effects of these parameters.

The steady flux of a fluid through unit area of a membrane is given by Fick's first law of diffusion,

$$J = -D \frac{\partial c}{\partial x} \tag{32}$$

where D is the diffusion coefficient and c is the concentration of fluid within the membrane, x being distance. The concentration can be approximated by Henry's law, $c = \alpha p$, where p is the fluid pressure, which will be vapor pressure at the temperature in question in the case of a liquid. Assuming also a constant concentration gradient through the entire thickness, d, of the membrane, then equation (32) can be written,

$$J = - \alpha D \, \Delta p/d \tag{33}$$

It is emphasized that Δp does not represent the total pressure drop across the membrane but only the decrease of partial pressure of fluid. Equation (32) is usually written

$$J = \Pi \, \Delta p/d \tag{34}$$

and Π is called the permeability constant. For the case of gases diffusing through various polymers (ref. 17) it has been found to depend exponentially on temperature:

$$\Pi = \Pi_o \exp [-E/RT] \tag{35}$$

where the temperature coefficient of E is of the order of 10 Kcal/mole.

The above model and analysis can be used to test the assertion that the permeation mechanism is primarily one of diffusion as distinguished from flow through micropores, and at the same time it provides an understanding of the experimental results which comprise the effects of the aforementioned influence parameters.

Consider first the predicted temperature dependence. An activated diffusion process will exhibit exponential temperature dependence. If, however, capillary flow prevails, and the fluid is a gas, the process will not exhibit very strong dependence on temperature. This is so because variation in the gas flow due to temperature change will only arise from gas density and viscosity changes. These properties show relatively weak dependences on temperature, which also happen to be opposed in direction. Hence the thermal dependence can sometimes help in deciding the controlling mechanism. When, however, the fluid is a liquid, the driving pressure for the capillary flow will be determined by the vapor pressure which also varies exponentially with temperature. This constitutes a severe limitation on the ability of temperature dependence to distinguish the mechanism. And to further complicate the problem, the temperature coefficient in the liquid case will be approximately the heat of vaporization which is of the order of 10 Kcal/mole for the halogenated organics of this study, the same as the previously-cited value for activated diffusion. Thus temperature dependence cannot decide between the permeation processes, but the observed dependence does follow as a logical consequence of either mechanism.

In contrast to the temperature parameter, the dependence of the process on external pressure can be used to distinguish the mechanism. Activated diffusion depends on the partial pressure drop of agent across the membrane wall, and quite secondarily on external pressure. Orifice or capillary flow on the other hand depends on the total pressure drop across the channel (to some power of pressure between 0.5 and 2.0), and hence significantly on external pressure. The general absence of total pressure dependence in the vacuum experiments is therefore not consistent with a flow process.

The thickness of the wall material is certainly expected to be an important parameter in containing agent within a capsule, and the present treatment provides an explanation. Equation (33) or (34) predicts that agent flux will be inversely proportional to membrane thickness simply because the concentration gradient flattens with longer diffusion distances. (If capillary flow were important, the channel length, i. e., wall thickness, is likewise inversely proportional to flux.) Experiments at National Cash

Register have demonstrated that agent release and wall thickness are inversely related, although the exact dependence was not determined.

For a given percent of agent in the microcapsule, wall thickness will increase and surface to volume ratio will decrease as the capsule size increases. These effects will tend to reduce agent loss by diffusion. However, if the particle size becomes too large the capsules will be more fragile and susceptible to thermal rupture, and they will be less suitable for incorporation into a plastic matrix. The choice of capsule size for a particular application will involve a compromise between opposing requirements.

It remains to discuss, in light of the model, the effect of the chemical nature of the agent and that of capsule material on permeation rate. Capillary or orifice flow does not depend on the molecular characteristics of the fluid, unless the pores are comparable in size to molecule dimensions. However, diffusion will substantially depend on the molecular properties of both agent and membrane. The interaction of polymer and agent can be discussed in terms of the solubility parameter δ or the related cohesive energy density E/V.

$$\delta = (E/V)^{1/2} \qquad (36)$$

Here E is the total cohesive energy (heat of evaporation) and V is the molar volume. Liquids with similar solubility parameters will show enhanced mutual solubility. The coehesive energy depends on dispersion forces, dipole interactions, and hydrogen bonding. Thus, while an agent and membrane material having similar degrees of polarity may be expected in general to show mutual solubility and good permeability, a variety of anomalous behaviors can be observed.

Diffusion through a polymeric membrane will be further affected by the physical structure of the polymer. Diffusion is usually slower through crystalline than through amorphous polymers. Cross linking will reduce the equilibrium solubility (swelling) of the liquid and so should reduce permeability. At temperatures above the glass transition temperature T_g, increased mobility of the polymer segments will favor rapid diffusion. The glass transition

temperature of polyvinyl alcohol is approximately 80°C, depending somewhat on the degree of crystallinity. Swelling by a liquid will lower T_g, but the hardening agents used in preparing the microcapsules may have an opposite effect. The gelatin wall material is probably highly crystalline and insolubilized by cross linking. It shows strong hydrogen bonding and will interact with, and hold tenaciously, water or other hydrogen bonding solvents. Consequently, anomalous diffusion behavior is to be expected. Determination of the structure and physical properties of the capsule wall materials, as modified by the encapsulation process, will be a necessary step in obtaining a more quantitative description of microcapsule permeation behavior.

Capsule rupture at high temperature follows a different course. As the capsule is heated both the liquid agent and the capsule wall will expand, but the coefficient of expansion of the liquid may be an order of magnitude greater than that of the wall material. With most plastics the resulting wall stress would be relieved by plastic flow at temperatures above T_g, but in the case of highly cross linked polymers such flow may not be possible. Capsule rupture may result, particularly in the case of agents of low volatility.

With agents of greater volatility, the internal pressure of the capsule will be equal to the vapor pressure which increases exponentially with the temperature. At some point in the heating cycle the vapor pressure may exceed the strength of the capsule wall and capsule rupture will result. Agent loss through diffusion will take place simultaneously and, if the rate of heating is slow, the agent may escape before the critical pressure is reached.

The tensile stress in the wall of a thin walled sphere subjected to internal pressurization is approximately

$$\sigma = \frac{r\,\Delta P}{2t} \tag{37}$$

where r is the radius of the sphere, t is the wall thickness and ΔP is the pressure differential across the wall.

For a typical case r may be 50μ, t 5μ, and σ =5 ΔP. Observations indicate that the vapor pressure at rupture may be of the order of 100-200 psi so σ will have a value of a few hundred to a few thousand psi, typical of polymeric materials. From equation 37 it is apparent that for a constant wall thickness the smaller capsules will withstand a greater internal pressure. However, if the agent content of the capsule is kept constant r/t is approximately constant and nothing is gained by going to smaller capsule sizes.

The response of the capsule wall material to an applied stress is highly complex, depending on the temperature and the physical structure of the polymer (crystallinity, cross linking, plasticization, etc.) (ref. 18). The response will also depend on the rate of application of the stress. Below T_g the response to a rapidly applied stress (rapid heating) will be almost purely elastic with no permanent deformation. Above T_g a retarded elastic response is observed and the capsule swells. The thinning of the wall section is compensated to some extent by orientation of the polymer molecules. At still higher temperatures a "softening point" is reached where the polymer behaves as a viscous liquid with little elastic response. Capsule expansion becomes rapid and catastrophic wall failure occurs.

Thus, the experimental observations of vapor release are in qualitative accord with theoretical expectations. A more quantitative correlation must await a more detailed characterization of the wall materials.

CONCLUSIONS AND RECOMMENDATIONS

The opposed jet-burner affords a convenient and meaningful method of evaluating fire extinguishing agents in a diffusion flame.

Many organohalogen compounds are effective fire suppressants when introduced into the fuel side of a diffusion flame.

Of a series of organohalogen agents evaluated by this technique, bromoform ($CHBr_3$) was found to be the most effective on a weight or volumetric basis. Its physical properties also appeared to be suitable for microencapsulation.

A high bromine content appears to be necessary for good efficiency in organohalogen type agents.

The fluorine containing agents CF_3Br, CF_2BrCF_2Br, and $CF_2ClCFCl_2$ were found to be less effective in the diffusion flame than in previous studies in premixed flames.

Significant differences in behavior are observed when the agent is introduced from the fuel side or the air side of the opposed jet burner. Further studies should contribute to an understanding of the mechanism of inhibition in diffusion flames.

A wide variety of chemical fire suppression agents are suitable for use in the microencapsulation technique. It is recommended that the screening of candidate agents be extended to include a wider range of chemical structures and compositions in a search for more efficient systems.

Polymeric microcapsules containing volatile fire suppressing agents lose agent slowly at low temperatures by a permeation process. The permeation rate depends on the chemical structure of the agent and encapsulant.

Polyvinyl alcohol is more effective than gelatin as an encapsulant in reducing the permeation rate for the agents studied.

Carbon tetrabromide diffuses readily through the capsule wall while the chemically similar but molecularly smaller $CBrCl_3$ is lost much more slowly. Despite its volatility (b. p. 47.6°C), $CF_2ClCFCl_2$ diffuses even more slowly.

Upon rapid heating (as when exposed to a fire), microcapsules rupture due to internal pressure and loss of physical strength in the wall material.

Capsules can withstand internal (vapor) pressure of the order of 100 to 200 psi before rupture. Observed tensile stresses in the wall at rupture are in qualitative agreement with expected properties of the wall materials.

The rate of permeation of agent through the capsule wall increases only slowly with increased temperature and internal pressure.

The samples of microcapsules examined in this program were quite heterogeneous with respect to size, wall thickness, and physical strength. A fraction of the capsules in a sample would rupture when heated to a relatively low temperature while others would withstand a much higher temperature.

It is recommended that a detailed study of the chemical structure and mechanical properties of the wall materials, as modified by the encapsulation process, be made to provide a basis for a more quantitative understanding of agent loss from microcapsules through permeation and capsule rupture.

REFERENCES

1. Potter, A. E.; and Butler, J. N.: A Novel Combustion Measurement Based on the Extinguishment of Diffusion Flames. ARS J., vol. 29, 1969, p. 54.

2. Potter, A. E.; Heimel, Sheldon; and Butler, James N.: A Measure of Maximum Reaction Rate in Diffusion Flames. Eighth Symposium (International) on Combustion. Williams and Wilkins, 1962.

3. Friedman, R.; and Levy, J. B.: Inhibition of Opposed-Jet Methane-Air Diffusion Flames. The Effects of Alkali Metal Vapors and Organic Halides. Combustion and Flame, vol. 7, 1963, p. 195.

4. McHale, Edward T.: Survey of Vapor Phase Chemical Agents for Combustion Suppression. NASA CR-73263, August, 1968.

5. Purdue University Foundation and Department of Chemistry: Final Report on Fire Extinguishing Agents for the Period 1 September 1947 to 30 June 1950. Purdue University, July, 1950.

6. Simmons, R. F.; and Wolfhard, H. G.: The Influence of Methyl Bromide on Flames. II - Diffusion Flames. Vol. 2, Trans. Faraday Soc., 1956, p. 53.

7. Creitz, E. C.: Inhibition of Diffusion Flames by Methyl Bromide and Trifluoromethyl Bromide Applied to the Fuel and Oxygen Sides of the Reaction Zone. J. Research, NBS, vol. 65A, 1961, p. 389.

8. Levy, A.; Droege, J. W.; Tighe, J. J.; and Foster, J. F.: The Inhibition of Lean Methane Flames. Eighth Symposium (International) on Combustion. Williams and Wilkins, 1962, p. 524.

9. Fenimore, C. P.; and Jones, G. W.: Flame Inhibition by Methyl Bromide. Combustion and Flame, vol. 7, 1963, p. 323.

10. Pandya, T. P.; and Weinberg, F. J.: The Structure of Flat, Counter-Flow Diffusion Flames. Proceedings of the Royal Society, A, vol. 279, 1964, pp. 544.561.

11. Fristrom, R. M.; and Westenberg, A. A.: Flame Structure. McGraw-Hill, 1965.

12. Rice, F. O.; and Rice K. K.: The Aliphatic Free Radicals. Johns Hopkins Press, 1935.

13. Lewis, B.; and von Elbe, G.: Combustion, Flames, and Explosions of Gases. Academic Press, 1961.

14. Wilson, W. E.: Structure, Kinetics, and Mechanism of a Methane-Oxygen Flame Inhibited with Methyl Bromide. Tenth Symposium (International) on Combustion, The Combustion Institute, 1966, p. 47.

15. Anderson, J. W.; and Friedman, R.: An Accurate Gas Metering System for Laminar Flow Studies. The Review of Scientific Instruments, vol. 20, no. 1, January, 1949, pp. 61-66.

16. Jost, W.: Diffusion in Solids, Liquids, Gases. Academic Press, New York, 1960.

17. Barrer, R. M.: Trans. Faraday Soc. Vol. 35, 1939, p. 628.

18. Alfrey, Turner, Jr.: High Polymers. Vol. VI. Interscience Publishers, Inc., 1948.

APPENDIX

Table AI

Flame Strength Measurements in the Opposed Jet Burner

Agent and Burner Temperature	Air Flow cc/sec	Propane Flow cc/sec	Agent Percent by Volume in Fuel	Flame Strength N_f
$CHBr_3$	12.54	7.57	0	1
	12.00	6.66	2.34	.880
200°C	12.43	6.38	4.85	.843
			5.40	unstable
CBr_4	13.87	8.02	0	1
	12.96	6.39	9.70	.797
220°C	13.64	7.89	0	1
	13.41	7.20	2.27	.912
	12.50	6.39	4.95	.810
	13.30	7.06	2.31	.895
	12.73	6.51	4.85	.825
CH_3Br	10.83	6.25	0	1
	10.85	5.51	5.14	.882
104°C	10.43	5.29	6.75	.846
	10.69	5.38	7.54	.861
	10.43	5.10	8.68	.816
	10.57	4.86	9.65	.778
CCl_3Br	9.19	5.24	0	1
	9.35	3.76	8.3	.718
112°C	9.53	5.24	0	1
	9.23	4.61	5.1	.880
	9.85	5.38	0	1
	10.15	4.94	3.8	.918
	9.94	5.53	0	1
	9.26	5.21	1.0	.942

Table AI Continued

Agent and Burner Temperature	Air Flow cc/sec	Propane Flow cc/sec	Agent Percent by Volume in Fuel	Flame Strength N_f
CCl_4	9.94	5.43	0	1
	10.03	5.29	2.41	.97[illegible]
112°C	9.94	5.15	2.47	.94[illegible]
	10.12	5.56	0	1
	9.69	5.05	4.5	.90[illegible]
	9.76	4.56	8.6	.78[illegible]
	10.65	5.84	0	1
	10.37	5.84	0	1
	10.72	5.42	5.0	.92[illegible]
	10.65	5.84	0	1
	9.76	4.56	8.6	.78[illegible]
	10.12	5.56	0	1
	9.69	4.99	4.5	.89[illegible]
	9.99	5.56	0	1
	9.62	5.10	4.0	.91[illegible]
CF_3Br	10.86	6.34	0	1
	11.48	5.91	5.83	..92[illegible]
110°C	10.24	4.75	11.63	.74[illegible]
	9.48	5.31	0	1
	9.25	4.31	13.11	.77[illegible]
	9.32	4.63	6.45	.87[illegible]
	9.89	5.37	0	1
	9.82	4.78	6.26	.89[illegible]
	9.71	4.48	9.16	.83[illegible]
	9.54	4.24	10.66	.79[illegible]
$C_2H_2Br_4$	13.41	8.16	0	1
	13.30	7.34	1.91	.93[illegible]
220°C	13.41	6.92	3.85	.84[illegible]
	13.87	6.80	7.68	.88[illegible]

Table AI Continued

Agent and Burner Temperature	Air Flow cc/sec	Propane Flow cc/sec	Agent Percent by Volume in Fuel	Flame Strength N_f
$C_2F_4Br_2$	12.65	7.43	0	1
	12.65	7.17	1.59	.965
200°C	12.87	7.04	3.27	.948
	12.00	7.16	0	1
	11.78	6.66	2.11	.930
	11.67	6.38	4.58	.891
	11.45	5.86	8.76	.818
Agent admixed to air			Percent in air	
	10.69	5.78	1.33	.924
	11.56	6.25	0	1
$C_2F_4Br_2$	7.38	4.57	0	1
	7.43	4.32	3.66	.945
60°C	7.50	4.07	7.56	.891
	7.43	3.64	15.12	.796
	7.71	3.56	18.96	.780
Agent admixed to air			Percent in air	
	7.47	4.47	0	1
	7.59	4.45	.46	.995
	7.38	4.36	.96	.975
	7.21	4.28	1.21	.957
	7.55	4.45	0	1
	7.27	4.36	1.13	.980
	5.76	3.43	2.77	.771
	59	4.53	0	1
	56	3.52	2.72	.777
			5.44	unstable
$C_2Cl_3F_3$	10.47	6.37	0	1
	10.12	6.05	7.0	.950
112°C	10.51	6.26	7.0	.983
	11.00	6.79	0	1
	10.44	6.47	6.5	.953
	10.88	6.58	6.5	.969
	10.76	6.26	11.7	.922
	10.44	6.16	11.7	.907
	11.01	5.73	18.0	.844
	11.04	5.52	22.4	.813

Table AI Concluded

Agent and Burner Temperature	Air Flow cc/sec	Propane Flow cc/sec	Agent Percent by Volume in Fuel	Flame Strength N_f
H_2O	12.11	6.28	0	1
	12.32	5.83	20.7	.928
180°C	12.32	5.17	11.1	.982
	12.53	6.34	0	1
	11.49	4.50	40.9	.710
	11.90	5.41	22.2	.853
111°C	9.47	5.04	0	1
	9.34	4.64	3.95	.921
	9.59	5.12	0	1
	9.49	4.93	3.11	.963
	9.34	5.18	0	1
	8.76	3.86	30.30	.745
	9.47	5.12	0	1
	9.65	4.93	14.2	.963
	9.56	5.23	0	1
	9.03	4.58	12.4	.876
	9.49	5.23	0	1
	9.24	4.74	10.75	.906
SO_2	9.89	5.22	0	1
	9.71	4.70	9.22	.900
117°C	9.80	4.45	14.50	.852
	10.16	5.25	0	1
	9.89	4.37	15.75	.832
	9.71	4.16	18.25	.792
	10.07	4.80	6.43	.914
Agent admixed to air			Percent in air	
25°C	7.34	5.00	0	1
	5.83	3.94	3.80	.788
	6.52	4.59	2.32	.902
	5.90	4.02	3.75	.804
	6.31	4.35	3.15	.870

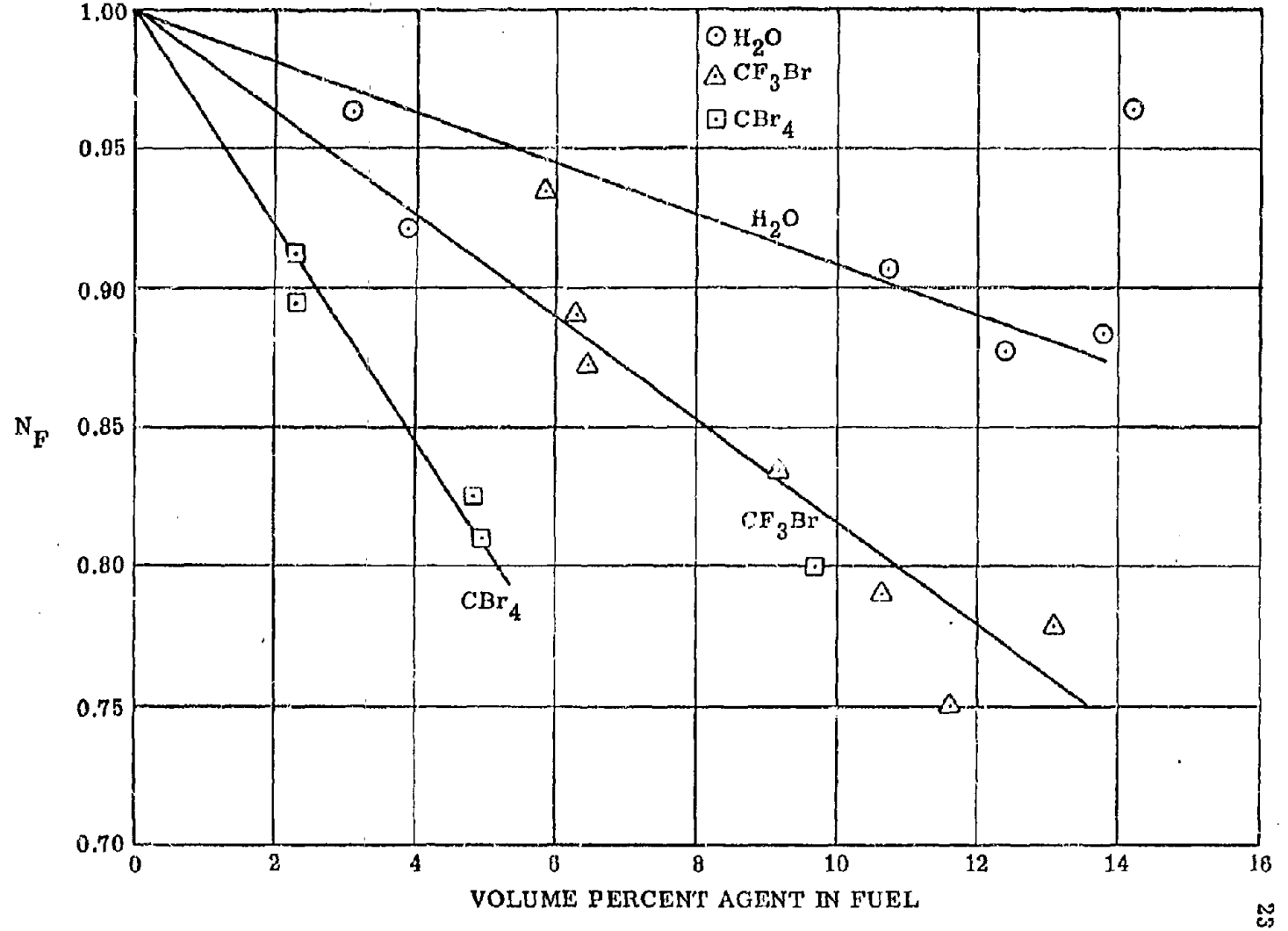

Figure AI. Plot of Measurements of Flame Strength Versus Agent Added to Fuel for Three Selected Inhibitors.

Table AII

Microencapsulated Extinguishing Agent
Furnished by the National Cash Register Co.

Sample No.	Agent	Wall Material	% Agent	Particle Size -u
Unknown	$CF_2ClCFCl_2$	Gelatin		
S-61168-1	$CBrCl_3$	Gelatin (Phenolic)[a]	87	50-105
J-61068-1	$CBrCl_3$	Polyvinylalcohol (Phenolic)[a]	96	53-177
S-61168-2	CBr_4	Gelatin (Phenolic)[a]	81	63-210
S-71568-1	Tris (2,3-dibromopropyl) phosphate	Polyvinylalcohol		
D-71268-1	Tris (2,3-dibromopropyl) phosphate	Gelatin		
J-72968-1	CF_2BrCF_2Br	Polyvinylalcohol (Phenolic)[a]	97	63-210
J-72568-1	CF_2BrCF_2Br	Gelatin	91	63-210
J-80168-1	CBr_4	Gelatin	91	63-210
S-72368-1	CI_4	Gelatin	89	63-297
D-80268-1	P-nitroaniline Bisulfate	Parlon S-20	89	63-210
J-81368-2	Tris (2,3-dibromopropyl) phosphate	Gelatin	79	63-210
J-80768-1	$CHBr_2CHBr_2$	Gelatin	94	63-210
J-80868-1	$CHBr_2CHBr_2$	Polyvinylalcohol (Phenolic)[a]	98	44-149
J-81468-1	CBr_4	Gelatin	67	63-210
S-111468	$Mo(CO)_6$			
S-111268	$Mo(CO)_6$			
S-111268-P	$Mo(CO)_6$			

[a]Secondary wall material added to harden wall and reduce permeation.